

# ENRICHMENT PROGRAM REPORT

## *In vitro* Cytoprotective Study of *Litsea oppositifolia* Bark Extract Against UVB Exposure

STUDY PROGRAM  
**Biotechnology**

Jason Yang  
19010070

Field Supervisor: apt. Pietradewi  
Hartrianti, M.Farm., PhD  
i3L Supervisor: Dr. Riahna Kembaren,  
M.Sc.

**RESEARCH REPORT**  
***In vitro* Cytoprotective Study of *Litsea oppositifolia***  
**Bark Extract Against UVB Exposure**



By  
Jason Yang  
19010070

Submitted to

i3L – Indonesia International Institute for Life Sciences  
School of Life Sciences

in partial fulfillment of the enrichment program for the Bachelor of Science in  
**Biotechnology**



Research Project Supervisor: Dr. Riahna Kembaren, M.Sc.  
Research Project Field Supervisor: apt. Pietradewi Hartrianti, M.Farm., PhD

Jakarta, Indonesia  
2022

**CERTIFICATE OF APPROVAL****INSTITUT BIO SCIENTIA INTERNASIONAL INDONESIA**

Jl. Pulomas Barat Kav. 88 Jakarta Timur 13210 Indonesia  
 +6221 295 67888, +6221 295 67899, +6221 296 17296  
 www.i3l.ac.id

**Certificate of Approval**

Student : Jason Yang

Cohort : 2019

Title of final thesis project : Studi sitoprotektif in vitro Ekstrak *Litsea oppositifolia* Terhadap Paparan UVB  
*in vitro Cytoprotective study of Litsea oppositifolia Extract Against UVB Exposure*

We hereby declare that this final thesis project is from student's own work. The final project/thesis has been read and presented to i3L's Examination Committee. The final project/thesis has been found to be satisfactory and accepted as part of the requirements needed to obtain an i3L bachelor's degree.

Names and signature of examination committee members present:

1	Thesis Supervisor	: Dr. Riahna B.K. , S.Si., M.Sc.	Approved
2	Lead Assessor	: Wided K. Ph.D.	Approved
3	Assessor 2	: Mario D.B. , S.P., M.Biotech(Adv)	Approved

Acknowledged by,

Head of Study Program,

Ihsan Tria Pramanda, S.Si., M.Sc.

This is a form-based authentication form, gaining access to this form is a method of signer validation, therefore, this form does not require a signature. Scan the QR code to verify the document validity.



## **COPYRIGHT NOTICE**

The contents of this report are protected by the International Copyright Law. Therefore, any unauthorized distribution, copying, and/or duplication of this report's contents without the author's knowledge is not permitted unless the author is acknowledged through proper quotations and citations in their respective work.

Copyright © 2022 Jason Yang

All rights reserved.

## STATEMENT OF ORIGINALITY

submitted to

**Indonesia International Institute of Life Sciences (i3L)**

I, Jason Yang, do herewith declare that the material contained in my EP research report entitled:

*“In vitro Cytoprotective Study of Litsea oppositifolia Bark Extract Against UVB Exposure”*

is original work performed by me under the guidance and advise of my EP Advisor, Dr. Riahna Kembaren, M.Sc., I have read and do understand the definition and information on use of source and citation style published by i3L. By signing this statement I unequivocally assert that the aforementioned thesis conforms to published information.

i3L has my permission to submit and electronic copy of my thesis to a commercial document screening service with my name included. If you check NO, your name will be removed prior to submission of the document for screening.

Yes

No

Name of student: Jason Yang

Student ID: 19010070

Study Program: Biotechnology



Signature:

Date: 22 December 2022

## ABSTRACT

Exposure of human skin to the sun has been known to have adverse effects. UV radiation, namely UVB (280-315 nm), is known to cause sunburn in the skin, as it induces cytokines, neuroactive, and vasoactive mediators that trigger an inflammatory response. Other than that, UV exposure is also linked with skin darkening, as it upregulates melanin accumulation in the epidermis. This increases the risk of melanoma in people. UV exposure also induces reactive oxygen species (ROS) in the skin. This study compares the *Litsea oppositifolia* bark extract as a potential solution that protects against UVB exposure, and its cytoprotective protective abilities were observed towards HaCaT cells. DPPH assay was performed, where it was observed that LO bark extract had an  $IC_{50}$  of  $48.660 \text{ ppm} \pm 3.97$ , which is weaker than ascorbic acid with an  $IC_{50}$  of  $3.853 \text{ ppm} \pm 2.27$ . The optimum UVB time and distance deemed cytotoxic to the cells was 6 hours from 15 cm. The extract was not cytotoxic to the cells, but ascorbic acid is cytotoxic from a concentration of 50 ppm. The cytoprotective assay showed that LO bark extract exhibited cytoprotective abilities at 100 ppm when exposed to UVB light. However, AA still had stronger cytoprotective abilities at lower concentrations, namely 25 and 50 ppm. Therefore, it was confirmed that LO bark extract exhibited antioxidant activity and cytoprotective abilities, although weaker when compared to AA.

Keywords: *Litsea oppositifolia*, UVB exposure

## ACKNOWLEDGEMENTS

First and foremost, I would like to express my utmost gratitude and worship to God Almighty, as through His guidance and blessings, this project was able to be completed. Other than that, I would also like to thank my EP advisor, Dr. Riahna Kembaren, M.Sc., and my field supervisor, apt. Pietradewi Hartrianti, M.Farm., PhD., for guiding me throughout the project, and without their guidance and support, this project would not have been possible.

I also would like to thank my research assistant, Erika Chriscensia, for assisting in procuring the materials needed for the experiment and my fellow project mates in the *Litsea oppositifolia* project, namely Crisshella Hana, Patricia Lovina, and Vivian Cherisa Arifin for assisting in taking care of the cells, helping in the process of the experiments and conducting preliminary studies used in this research.

Lastly, I would like to thank my family members, friends, lab assistants, staff members, assessors, and countless people who have helped assist with the project. It is because of their assistance that the project is as it is today.

## TABLE OF CONTENTS

<b>CERTIFICATE OF APPROVAL</b>	<b>ii</b>
<b>COPYRIGHT NOTICE</b>	<b>iii</b>
<b>STATEMENT OF ORIGINALITY</b>	<b>iv</b>
<b>ABSTRACT</b>	<b>v</b>
<b>ACKNOWLEDGEMENTS</b>	<b>vi</b>
<b>TABLE OF CONTENTS</b>	<b>vii</b>
<b>LIST OF FIGURES, TABLES, AND ILLUSTRATIONS</b>	<b>ix</b>
<b>LIST OF ABBREVIATIONS</b>	<b>xi</b>
<b>CHAPTER 1: INTRODUCTION</b>	<b>1</b>
1.1 Background	1
1.2 Research Questions	2
1.3 Objective	2
1.4 Scope of Research	3
1.5 Hypothesis	3
<b>CHAPTER 2: LITERATURE REVIEW</b>	<b>4</b>
2.1 <i>Litsea oppositifolia</i>	4
2.2 Oxidative damage UVB radiation	5
2.2.1 UVB radiation	5
2.2.2 Oxidative damage of ROS	6
2.3 HaCaT cell	7
2.3.1 Human Skin	7
2.3.2 HaCaT cells	7
2.4 Antioxidants	8
2.4.1 Ascorbic Acid	8
2.4.2 2,2-diphenyl-1-picrylhydrazyl (DPPH) Assay	8
2.5 Phytochemicals	9
2.5.1 Flavonoid	9
2.5.2 Tannin and Phenolic	10
2.5.3 Alkaloid	10
2.5.4 Saponin	10
<b>CHAPTER 3: MATERIALS &amp; METHODS</b>	<b>11</b>
3.1. Materials	11
3.2 Characterisation of the <i>Litsea oppositifolia</i> extract	11
3.2.1 Phytochemical screening	11



3.2.1.1 Flavonoid	11
3.2.1.2 Tannin & Phenolic	11
3.2.1.3 Alkaloid	11
3.2.1.4 Saponin	12
3.2.2 Total Phenolic Content (TPC)	12
3.2.3 Total Flavonoid Content (TFC)	12
3.2.4 Total Alkaloid Content (TAC)	13
3.2.5 2,2-diphenyl-1-picrylhydrazyl (DPPH) Assay	13
3.3 In vitro testing in HaCaT cells	14
3.3.1 HaCaT cell culture	14
3.3.2 UVB light exposure optimization	15
3.3.3 Cytotoxicity assay of <i>Litsea oppositifolia</i> extracts and ascorbic acid	15
3.3.4 Cytoprotective assay	16
<b>CHAPTER 4: RESULTS AND DISCUSSION</b>	<b>18</b>
4.1 <i>Litsea oppositifolia</i> bark extract characterization	18
4.1.1 Phytochemical screening	18
4.1.2 Total Phenolic Content	19
4.1.3 Total Flavonoid Content	20
4.1.4 Total Alkaloid Content	21
4.1.5 2,2-diphenyl-1-picrylhydrazyl (DPPH) Assay	22
4.2 In vitro assay in HaCaT cell	23
4.2.1 UVB light irradiation optimization	23
4.2.2 Cytotoxic assay	27
4.2.3 Cytoprotective assay	29
<b>CHAPTER 5: CONCLUSION AND RECOMMENDATIONS</b>	<b>32</b>
<b>REFERENCES</b>	<b>33</b>
<b>APPENDICES</b>	<b>38</b>

## LIST OF FIGURES, TABLES, AND ILLUSTRATIONS

- Figure 2.1** *Litsea oppositifolia* plant (Rohwer, 2013).
- Figure 2.2** Diagram of UV radiation. UVB penetrates to the epidermis, UVA penetrates deep into the dermis, and UVC is blocked by the ozone layer.
- Figure 2.3** Cultured Human Immortalised Keratinocytes (HaCaT) cells.
- Figure 2.4** Mechanism of the reaction of DPPH molecules against an antioxidant. R:H represents an antioxidant molecule, whereas R• represents an antioxidant radical (Liang & Kitts, 2014)
- Figure 3.1** 96-well plate map for DPPH Assay. The treatments are DPPH + methanol (blank; green), DPPH + LO extract at different ppm (blue), and DPPH + AA at different ppm (purple). Concentration of DPPH + LO from top to bottom: 1000, 500, 250, 125, 62.5, 31.25, 15.625, and 7.8125 ppm; concentration of DPPH + AA from top to bottom: 100, 50, 25, 12.5, 6.125, and 3.125 ppm.
- Figure 3.2** 96-well plate for the cytotoxic assay. The treatments include: cDMEM only (blank; green), cells + cDMEM only (negative control; orange), cells + media + LO extract at different ppm (blue), and cells + media + AA at different ppm (purple). Concentration is decreasing from the top for LO and AA treatments (200, 100, 50, 25, 12.5, 6.25 ppm).
- Figure 3.3** 96-well plate for the cytoprotective assay. The treatments include: cDMEM only (blank; green), cells + cDMEM only (negative control; orange), cells + media + LO extract at different ppm (blue), and cells + media + AA at different ppm (purple), the concentrations for blue and purple were decided from the cytotoxicity test, where concentrations deemed cytotoxic from the cytotoxic assay were omitted for this analysis.
- Table 4.1** Phytochemical screening result of LO bark extract. “+” indicates a positive result, while “-” indicates a negative result.
- Figure 4.1** Total Phenolic Content quantification of LO extract against quercetin as a standard. Black circle: Gallic acid standard curve absorbances; Blue square: LO extract absorbance; Standard curve equation:  $y: 0.007155x + 0.03298$ , R squared value: 0.9712; p-value: <0.0001.
- Figure 4.2** Total Flavonoid Content quantification of LO extract against quercetin as a standard. Black circle: Quercetin standard curve absorbances; Blue square: LO extract absorbance; Standard curve equation:  $y: 0.0033139x + 0.0274$ , R squared value: 0.9867; p-value: <0.0001.
- Figure 4.3** Total Alkaloid Content quantification of LO extract against quercetin as a standard. Black circle: Atropine standard curve absorbances; Blue square: LO extract absorbance; Standard curve equation:  $y: 0.001021x + 0.04058$ , R squared value: 0.9111; p-value: <0.0001.

- Figure 4.4** DPPH assay results of LO bark extract (blue) and Ascorbic acid (black). R squared value LO extract: 0.9660; R squared value Ascorbic Acid: 0.9946.
- Figure 4.5** MTT Assay mechanism (Kamiloglu et al., 2020)
- Figure 4.6** UVB Irradiation optimization of HaCaT cells at 3 hours. The data is presented as mean  $\pm$  standard deviation. Black: Control (did not undergo UV irradiation); Orange: Underwent UV irradiation from a distance of 10 cm. Yellow: Underwent UV irradiation from a distance of 15 cm.
- Figure 4.7** UVB Irradiation optimization of HaCaT cells at 6 hours. The data is presented as mean  $\pm$  standard deviation. Black: Control (did not undergo UV irradiation); Orange: Underwent UV irradiation from a distance of 10 cm. Yellow: Underwent UV irradiation from a distance of 15 cm.
- Figure 4.8** UVB Irradiation optimization of HaCaT cells at 24 hours. The data is presented as mean  $\pm$  standard deviation. Black: Control (did not undergo UV irradiation); Orange: Underwent UV irradiation from a distance of 10 cm. Yellow: Underwent UV irradiation from a distance of 15 cm.
- Figure 4.9** Cell viability of HaCaT cells when treated with LO bark extract after 6 hours of incubation. The data is presented as mean  $\pm$  standard deviation. Black: negative control (cells with no treatment); Concentrations of LO bark extract is increasing from dark blue to light blue.
- Figure 4.10** Cell viability of HaCaT cells when treated with ascorbic acid after 6 hours of incubation. The data is presented as mean  $\pm$  standard deviation. Black: negative control (cells with no treatment); Concentrations of ascorbic acid are increasing from dark purple to light purple.
- Figure 4.11** Cytoprotective assay results of LO bark extract after six hours of UVB incubation time from a distance of 15 cm towards HaCaT cells. The data is presented as mean  $\pm$  standard deviation. Black: negative control (did not enter UV box); Grey: untreated cells irradiated with UV. Concentrations of LO bark extract is increasing from dark blue to light blue. \* indicates statistical significant difference against the negative control ( $P < 0.05$ ). \*\*\*\* indicates a statistical significant difference against the negative control ( $P < 0.0001$ ).
- Figure 4.12** Cytoprotective assay results of ascorbic acid after six hours of UVB incubation time from a distance of 15 cm towards HaCaT cells. The data is presented as mean  $\pm$  standard deviation. Black: negative control (did not enter UV box); Grey: untreated cells irradiated with UV. Concentrations of ascorbic acid are increasing from dark purple to light purple. \* indicates statistical significant difference against the negative control ( $P < 0.05$ ). \*\* indicates a statistical significant difference against the negative control ( $P < 0.01$ ).

## LIST OF ABBREVIATIONS

<b>AA</b>	Ascorbic Acid
<b>AE</b>	Atropine Equivalent
<b>BCG</b>	Bromocresol Green
<b>cdMEM</b>	Complete Dulbecco's Modified Eagle Medium
<b>CPD</b>	Cyclobutane pyrimidine dimers
<b>DMEM</b>	Dulbecco's Modified Eagle Medium
<b>DNA</b>	Deoxyribonucleic acid
<b>DPPH</b>	2,2-diphenyl-1-picrylhydrazyl
<b>FBS</b>	Fetal Bovine Serum
<b>GAE</b>	Gallic Acid Equivalent
<b>HaCaT</b>	Cultured Human Immortalised Keratinocytes
<b>HAT</b>	Hydrogen atom transfer
<b>IC<sub>50</sub></b>	Half maximal inhibitory concentration
<b>LO</b>	<i>Litsea oppositifolia</i>
<b>MMP</b>	Matrix metalloproteinases
<b>MTT</b>	3-[4,5-dimethylthiazol-2-yl]-2,5 diphenyl tetrazolium bromide
<b>Pen-strep</b>	Penicillin-streptomycin
<b>QE</b>	Quercetin Equivalent
<b>ROS</b>	Reactive Oxygen Species
<b>SET</b>	Single electron transfer
<b>UV</b>	Ultraviolet
<b>UVA</b>	Ultraviolet A
<b>UVB</b>	Ultraviolet B
<b>UVC</b>	Ultraviolet C
<b>TAC</b>	Total Alkaloid Content

## CHAPTER 1: INTRODUCTION

### 1.1 Background

The human skin is the largest organ in the human body, which acts as a physical barrier that protects the body's internal organs from external stressors (Swann, 2010; Karapetsas et al., 2020). These stressors range from pathogens, allergens, pollutants, and ultraviolet (UV) radiation (Karapetsas et al., 2020). As one of the sources of radiation, sunlight emits a broad spectrum of radiation, 3%-7% of which is UV radiation, 53% of infrared radiation, and 44% of visible light (Bernstein, Sarkas, & Boland, 2021; D'Orazio et al., 2013). Visible light is the light seen by the human eye; infrared light is felt as heat, whereas UV light cannot be felt or seen (US EPA, 2022). UV exposure has several benefits to the body, including vitamin D induction, suppression of multiple sclerosis symptoms, and synthesis of endorphins (Juzeniene & Moan, 2012; D'Orazio et al., 2013). However, overexposure to UV light could also pose a health risk. It is classified as a mutagen and a non-specific damaging agent, acting as a tumor promoter and initiator (D'Orazio et al., 2013).

UV radiation can be classified into three different types based on its wavelengths: ultraviolet A (UVA), ultraviolet B (UVB), and ultraviolet C (UVC) (Han et al., 2021; Karapetsas et al., 2020). UVA is the longest in wavelength (320-400 nm), followed by UVB (290-320 nm) and UVC (100-290 nm) (Han et al., 2021). Although UVC is the most damaging due to its short and intense wavelength, only UVA and UVB are responsible for skin damage as UVC is too short and is absorbed by the ozone layer (Karapetsas et al., 2020; Wilson et al., 2012). On the other hand, UVB can only penetrate the epidermis, while UVA penetrates deep into the dermis (Wang et al., 2019). Other than sunlight, there are other sources of UV, where artificial sources like tanning beds are used for people to expose themselves to UV rays (Gallagher et al., 2010). Due to the lack of regulation regarding tanning beds, UV output from tanning beds could reach up to ten times the strength of sunlight (D'Orazio et al., 2013). Prolonged exposure to UV rays causes significant damage to the skin, as the rays do not penetrate the skin's epidermis, increasing the risk of melanoma (Wilson et al., 2012; D'Orazio et al., 2013).

UVB radiation causes solar erythema, known as sunburn, as its waves induce cytokines, neuroactive, and vasoactive mediators in the skin that trigger an inflammatory response (D'Orazio et al., 2013). In addition, the damage caused by UVB radiation promotes p53 activation, thus eliminating the keratinocytes utilizing apoptosis for DNA repair. Other than that, UVB exposure is also linked with skin darkening, as it upregulates melanin accumulation in the epidermis, which increases the risk of melanoma in people (Gallagher et al., 2010; D'Orazio et al., 2013). UV exposure also

induces reactive oxygen species (ROS) formation in the skin, which leads to photoaging (Han et al., 2021; Karapetsas et al., 2021). Increased oxidative stress damages protein by direct oxidation, causing alterations in its structure and function, which results in the loss of enzymatic activity and protein functions (Perluigi et al., 2010).hannah

In protecting itself against ROS, the skin produces antioxidants, which could suppress ROS free radicals from harming the skin (Narendhirakannan & Hannah, 2013). For example, melanin is an antioxidant produced by the skin capable of absorbing UV rays and removing ROS from the body (Brenner & Herring, 2008). Other than that, the meals consumed daily could contain natural antioxidants, including vitamins C and E. Vitamin C, familiarly known as Ascorbic Acid (AA), is a micronutrient essential in protecting the skin from oxidative damage by donating electrons to the ROS free radicals, which further suppresses inflammatory tissue responses caused by these ROS, protecting the skin from further damage and photoaging (Fernández-García, 2014; Pehlivan, 2017; Angjaya, 2022). However, the antioxidants in the skin could deplete and may take 24 hours to restore endogenously (Coats et al., 2020). Furthermore, if the concentration of ROS is too high, these antioxidants would be overwhelmed, and oxidative damage would still occur (Narendhirakannan & Hannah, 2013). Because of these reasons, a component that contains antioxidants and UVB-absorbing properties that could be exogenously administered to protect the skin is required.

The bark extract obtained from the *Litsea oppositifolia* (LO) plant of the *Litsea* genus is a promising candidate for its antioxidative properties. However, more study still needs to be done on the plant, albeit known as a medicinal plant (Zakhrifah, 2019). Other *Litsea* plants, namely *Litsea elliptica* and *Litsea resinosa*, have been tested for their antioxidant properties and have shown high antioxidant properties (Wong et al., 2014).

## 1.2 Research Questions

The research questions for this research are as follows:

- Does the LO bark extract have antioxidant properties?
- Does the LO bark extract exhibit cytoprotective abilities toward the skin against UVB irradiation *in vitro*?
- Are the cytoprotective abilities of the LO bark extract better towards the skin against UVB irradiation *in vitro* in comparison to Ascorbic Acid?

## 1.3 Objective

This research was conducted to characterize LO bark extract using total flavonoid, phenolic, alkaloid contents, 2,2-diphenyl-1-picrylhydrazyl (DPPH) assay, and phytochemical screening.

Furthermore, this research aimed to analyze the characterized *Litsea oppositifolia* extract's cytoprotective abilities towards the skin in different concentrations against UVB irradiation *in vitro*.

#### 1.4 Scope of Research

The scope of this research includes the following:

- Characterization of *Litsea oppositifolia* extracts, which includes total phenolic content (TPC), total flavonoid content (TFC), total alkaloid content (TAC), DPPH assay, and phytochemical screening
- HaCaT cell culture
- UVB light exposure optimization test against cell death
- Cytotoxic assay of *Litsea oppositifolia* extracts and Ascorbic acid
- Cytoprotective assay by UVB irradiation
- Cell viability tests using 3-[4,5-dimethylthiazol-2-yl]-2,5 diphenyl tetrazolium bromide (MTT) assay

#### 1.5 Hypothesis

The hypotheses for this research are as follows:

- The LO bark extract has antioxidant properties.
- The LO bark extract exhibits cytoprotective abilities toward the skin against UVB irradiation *in vitro* and is better than Ascorbic Acid.

## CHAPTER 2: LITERATURE REVIEW

### 2.1 *Litsea oppositifolia*

*Litsea* is a genus of evergreen trees of the *Lauraceae* family found across tropical and subtropical regions (Kong et al., 2015). *Litsea* plants have many utilisations. Its plants have been known to exert several benefits in medicine. Twenty genera are used in traditional Chinese medicine as medication for diseases including diarrhea, diabetes, gastroenteritis, asthma, and many more (Kong et al., 2015). An example of such a plant is *Litsea cubeba*, found around the Himalayas (Kamle et al., 2019). The extracts from *Litsea plants* have been found to contain antimicrobial and anti-inflammatory properties, which aid in the cytoprotective abilities against ROS (Kong et al., 2015). Previous research has tested several *Litsea* plants for antioxidative properties, namely *Litsea elliptica* and *Litsea resinosa*, where they have been found to contain high antioxidative properties (Wong et al., 2014)

*Litsea oppositifolia* (seen in Figure 2.1) is a plant from the family *Lauraceae* native to Borneo and is known for its broad, opposite leaves larger than 8 cm with a midrib prominent above (Forest Research Institute Malaysia, 2005; Royal Botanic Gardens Kew, 2022). According to Global Biodiversity Information Facility (2017), the taxonomy for *Litsea oppositifolia* plant is as follows:

Kingdom: Plantae

Phylum: Tracheophyta

Class: Magnoliopsida

Order: Laurales

Family: Lauraceae

Genus: *Litsea* Lam.

Species: *Litsea oppositifolia* Gibbs.

*Litsea* is familiarly known in Indonesia as Phoebe (*Medang*) (Tamin, Ulfa, & Saleh, 2018). The plant has an elliptical and ovoid small drupe fruit with either an undeveloped or a small cup hypanthium either with or without pedicellate (Forest Research Institute Malaysia, 2005; Tamin, et a., 2018). Because of the antioxidative properties of other *Litsea* plants, *Litsea oppositifolia* is a promising candidate for its antioxidative testing; therefore, its bark extract was measured for its cytoprotective abilities against UVB irradiation.





**Figure 2.1.** *Litsea oppositifolia* plant (Rohwer, 2013).

## 2.2 Oxidative damage UVB radiation

### 2.2.1 UVB radiation

UVB radiation (seen in Figure 2.2) is one of the radiations emitted by the sun, with a wavelength ranging between 290 nm to 320 nm and accounting for 5-10% of all UV exposure (Han et al., 2021). UVB could also be found in tanning beds, which due to lack of regulations, could expose people to 10 times the strength of sunlight (D’Orazio et al., 2013). In addition, its wavelength can penetrate the ozone layer, unlike UVC, although it does not penetrate through the skin’s dermis like UVA rays (Wang et al., 2019).

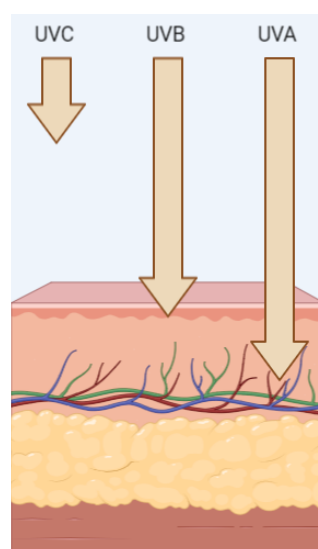


**Figure 2.2.** Diagram of UV radiation. UVB penetrates to the epidermis, UVA penetrates deep into the dermis, and UVC is blocked by the ozone layer.

UVB radiation causes damage to the skin, especially in the basal region of the epidermis, by inducing reactive oxygen species (ROS), which causes oxidative stress and damage to the biomolecules (Han et al., 2021; Karapetsas et al., 2020). The damages caused by barriers would result in skin drying, aging, and melanoma (Han et al., 2021). In addition, oxidative stress from UVB exposure leads to mitochondria-mediated apoptosis and damages proteins by altering their structure and function, which results in the loss of enzymatic activity and protein functions (Han et al., 2021; Perluigi et al., 2010). Furthermore, UVB radiation also forms UV-induced DNA photoproducts, cyclobutane pyrimidine dimers (CPDs), and pyrimidine 6-4 pyrimidines, inhibiting DNA replication and transcription that results in cell death and photoaging (Karapetsas et al., 2020). The same author also mentioned that UVB exposure could result in collagen degradation by inhibiting pro-collagen biosynthesis and the upregulation of matrix metalloproteinases (MMPs). These enzymes play an essential role in tissue remodeling and aging.

UVB radiation also causes solar erythema, familiar as sunburn, due to the induction of cytokines, neuroactive and vasoactive mediators in the skin that trigger an inflammatory response (D’Orazio et al., 2013). In addition, the damage caused by UVB radiation promotes p53 activation, thus eliminating the keratinocytes through apoptosis for DNA repair and increasing the risk of melanoma (D’Orazio et al., 2013; Han et al., 2021). Besides that, UVB exposure is also linked with skin darkening, as the upregulation of melanin accumulates in the epidermis, increasing the risk of skin cancer in people (Gallagher et al., 2010; D’Orazio et al., 2013).

### **2.2.2 Oxidative damage of ROS**

Reactive oxygen species (ROS) is a reactive molecule that is derived from the reduction of oxygen ( $O_2$ ) molecules into free radicals that include anion superoxides ( $O_2^-$ ), ozone ( $O_3$ ), and nitric oxides ( $NO\cdot$ ) (Beckhauser et al., 2016; Chriscensia, 2022). One of these compounds, hydrogen peroxide ( $H_2O_2$ ), when reduced, produces a hydroxyl radical ( $OH\cdot$ ) or water. The hydroxyl radical can remove electrons from other molecules, altering them into other free radicals and generating ROS (Beckhauser et al., 2016). In addition, ROS could be generated from the body’s metabolism, chemical reactions, and external sources, where these radicals diffuse into the nucleus to interact with the DNA (Beckhauser et al., 2016). One of these sources of ROS is UVB radiation, which could induce oxidative stress on the skin. Oxidative stress on the skin results in collagen degradation that affects tissue regeneration and aging. In order to combat these ROS from damaging the body, the skin has its defense mechanism against these ROS, where they produce antioxidants to absorb these radiations and remove ROS from the body in the form of melanin (Narendhirakannan &

Hannah, 2013; Han et al., 2021; Karapetsas et al., 2020). However, accumulating these will cause oxidative damage, inducing photoaging and melanoma.

## 2.3 HaCaT cell

### 2.3.1 Human Skin

The human skin is the largest organ of the human body, making up 16% of the body mass (D'Orazio et al., 2013). It is the body's external physical barrier, protecting it from external pathogens and environmental stresses, including UV exposure. The skin is also involved in homeostasis, regulating the temperature and moisture of the skin. The skin comprises three layers, the epidermis, the dermis, and the hypodermis (Yousef et al., 2021). However, UVB waves can only penetrate the skin's epidermis, in the basal region, *stratum basale*, which is the deepest layer of the epidermis (Yousef, Alhaji, & Sharma, 2021; Wang et al., 2019). There are also several skin cell types: keratinocytes, melanocytes, Langerhans, and Merkel cells (Yousef et al., 2021).

Keratinocytes are the dominant cells in the epidermis, which originate from the *stratum basale*, and are responsible for keratin production and the regulation of calcium absorption of UVB light in order to form vitamin D. Melanocytes, also found in the *stratum basale* of the epidermis, produce melanin that acts as an antioxidant when UVB exposure stimulates the secretion of the melanin. Langerhans' cells, also known as dendritic cells, are responsible for antigen preservation and the immune system. Lastly, Merkel cells are oval-shaped cells in the *stratum basale* that act as sensory receptors (Yousef et al., 2021).

### 2.3.2 HaCaT cells

As UVB exposure affects the skin, mainly the keratinocytes cell of the *stratum basale*, keratinocyte cells are favorable for the *in vitro* cryoprotective studies of the extract. Cultured Human Immortalised Keratinocytes, familiarly known as HaCaT cells, are non-tumorigenic monoclonal cell lines that could be used for studies of skin biology and differentiation (Colombo et al., 2012; Wilson, 2013). HaCaT cells are favored in this research because of their immortalized nature and high cell density. In addition, they are proven to be similar to keratinocytes in the skin in the production of cytokines (Colombo et al., 2012; Wilson, 2013). Although other cell lines, like the typical human epidermal keratinocytes, exist, these cells are not immortal, so they have a limited passage number (Adiyanto, 2022).

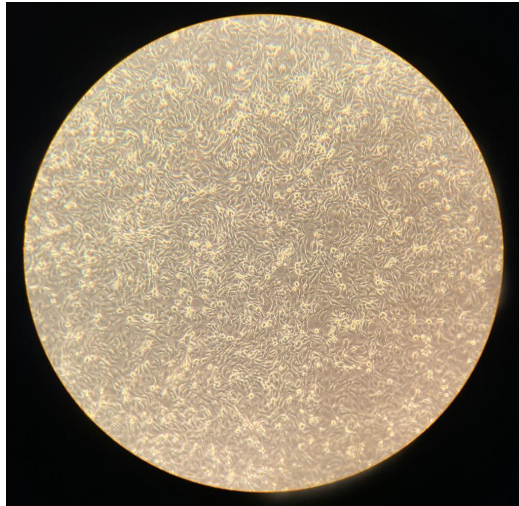


**Figure 2.3.** Cultured Human Immortalised Keratinocytes (HaCaT) cells.

## **2.4 Antioxidants**

The skin produces antioxidants in the form of melanin to protect itself from UV damage. However, these can be depleted and require an exogenous source to replenish and prevent the skin from oxidative damage.

### **2.4.1 Ascorbic Acid**

Ascorbic acid (AA), known as Vitamin C, is a micronutrient with antioxidant abilities against UV irradiation (Fernández-García, 2014). AA is an essential nutrient required for human growth, collagen hydroxylation, and amidation of peptides, among others (Angjaya, 2022). In addition, AA can protect the skin from oxidative stress by donating electrons to the free radicals by targeting ROS and suppressing inflammatory tissue responses (Fernández-García, 2014; Pehlivan, 2017). Food items containing AA and phenolic compounds also contribute to endogenous photoprotection, where using these micronutrients could aid in preventing the skin from UVB irradiation damage. Because of these reasons, AA is chosen as a comparator for the cytoprotective abilities of the LO bark extract against UVB irradiation.

### **2.4.2 2,2-diphenyl-1-picrylhydrazyl (DPPH) Assay**

There are two ways that the antioxidants react with the free radicals, which are through hydrogen atom transfer (HAT), or single electron transfer (SET) reactions (Liang & Kitts, 2014). The HAT reaction involves the removal of the hydrogen electron of the antioxidant, making the antioxidant a radical, whereas in a SET reaction, which the DPPH reaction mechanism is based on,

utilizes single electron is transfer from the nucleophile to the substrate, making the antioxidant a radical cation (Liang & Kitts, 2014).

DPPH assay is a method of testing the antioxidant activity of the assay first developed by Blois in 1958 (Kedare & Singh, 2011). DPPH acts upon free radicals in a way that binds the molecule to a free radical from ROS and reduces it, resulting in the color change from a deep violet color into a colorless solution, which is seen in Figure 2.4 (Nagarajan et al., 2006; Garcia et al., 2012). This testing method is most commonly used for plant and fruit extracts, making it suitable for testing the activity of LO bark extract (Nagarajan et al., 2017; Kedare & Singh, 2011). Another reason that the DPPH assay is suitable to test the antioxidant properties of the LO extract is due to its simple, rapid, inexpensive, and commonly used method in the testing of free radical activity of various samples because of its stable, quick, and its ability to react with weaker antioxidants; allowing to assess several samples at a time (Kedare & Singh, 2011; Garcia et al., 2012).

The DPPH solution is a stable free radical violet in color at room temperature (Kedare & Singh, 2011; Garcia et al., 2012). DPPH assay relies on the free radical scavenging activity of antioxidants towards the solution, where the free radical in the antioxidants utilizes electron transfer to reduce the nitrogen in the DPPH solution, turning the DPPH solution clear (Garcia et al., 2012; Kedare & Singh, 2011). The presence of antioxidants will reduce the 2,2-diphenyl-1-picrylhydrazyl compound into 1,1-diphenyl-1-picrylhydrazyl (Angjaya, 2022).

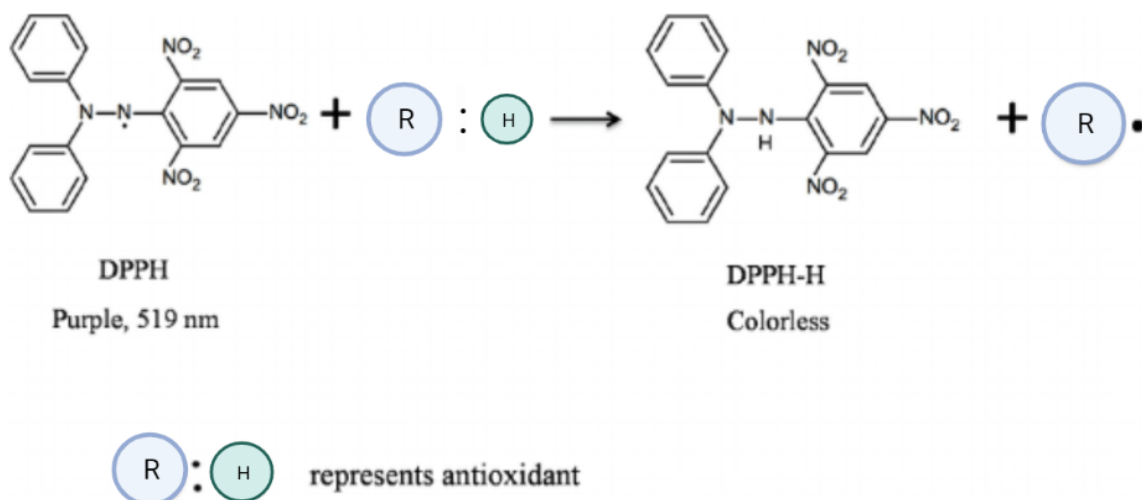


**Figure 2.4.** Mechanism of the reaction of DPPH molecules against an antioxidant. R:H represents an antioxidant molecule, whereas R• represents an antioxidant radical (Liang & Kitts, 2014)

## 2.5 Phytochemicals

### 2.5.1 Flavonoid

Flavonoids are one of the phytochemicals ubiquitously present in various fruits and vegetables, along with plant barks, leaves, and other parts of plants (Panche et al., 2016; Kumar &

Pandey, 2013; Ullah et al., 2020). They are polyphenolic compounds containing a benzopyrone structure in different positions (Panche et al., 2016; Kumar & Pandey, 2013). Flavonoids are utilized in skincare products, cosmetics, and dyes due to their beneficial properties (Ullah et al., 2020). Flavonoids possess antimicrobial, antioxidant, anti-inflammatory, and anticarcinogenic properties (Panche et al., 2016; Kumar & Pandey, 2013). Its antioxidant properties can be seen in plant tissues, as it defends tissues exposed to abiotic and biotic stresses (Kumar & Pandey, 2013). Furthermore, its antioxidant properties were found in high levels in both *in vitro* and *in vivo* systems (Kumar & Pandey, 2013). Because of this, the presence of flavonoids is desired in LO extract.

### **2.5.2 Tannin and Phenolic**

Tannins are complex phenolic compounds in various plants that can remove unstable proteins by utilizing hydrogen bonding (Basheer et al., 2022). They are known through their structure, which contains two to three phenolic hydroxyl groups on a phenyl ring (Okuda & Itto, 2011). In addition, phenolic compounds are known to possess polyphenolic properties, which include anticarcinogenic, antimicrobial, and antioxidant activities, where they can protect cells from oxidative damage caused by ROS (Chung et al., 1998; Okuda & Itto, 2011). Polyphenols could also help defend against UV irradiation (Kupina et al., 2018). As phenolic compounds are vital components in antiaging, anti-inflammatory responses, and antioxidant activities, the presence of tannin and phenolic compounds are desired in the LO extract (Lin et al., 2021).

### **2.5.3 Alkaloid**

Alkaloids are nitrogen-containing compounds derived from amino acids isolated from plants (Ferreira, 2022; Heinrich et al., 2021). They are known for their antiviral, anti-inflammatory, and anticancer properties in treating various human diseases (Ferreira, 2022; Kurek, 2019). In addition, alkaloids also have a potential for antioxidant activities, which could be further developed (Dey et al., 2020). Because of this, alkaloids in LO extract could also prove beneficial in protecting the skin against oxidative stress caused by UVB exposure.

### **2.5.4 Saponin**

Saponins are steroidal, and triterpene glycosides are found naturally in plants (Mugford & Osbourn, 2012). Its name is due to the soaplike properties of the compound (Mugford & Osbourn, 2012). They play a role in plant defense due to their antimicrobial, anticarcinogenic, anti-inflammatory, antifungal, antiparasitic, and antifeedant properties (Moses et al., 2014). Because of this, saponins play a role in the defense against cardiovascular diseases (Singh & Chaudhuri, 2018). Saponins are desired in LO extract due to their anti-inflammatory properties.

## CHAPTER 3: MATERIALS & METHODS

### 3.1. Materials

The *Litsea oppositifolia* bark extract was provided by the Department of Pharmacy of the University of Indonesia. This *Litsea oppositifolia* bark extract was obtained by maceration using ethanol as a solvent. The final result of extraction is in the form of paste with a mass of 2.5 grams. The reagent of 3-(4,5-Dimethylthiazol-2-yl)-2,5-Diphenyltetrazolium Bromide (MTT) for cell viability assay was purchased from Thermo Fisher Scientific.

### 3.2 Characterisation of the *Litsea oppositifolia* extract

#### 3.2.1 Phytochemical screening

The LO bark extract was diluted in type III (distilled) water into a concentration of 2000 parts per million (ppm) for the phytochemical screening of the extract. Phytochemical screening of the LO bark was obtained from a preliminary study using the same bulk of extract. As the screening of the phytochemicals is qualitative, the assays were performed in monoplicate. Therefore, only phytochemicals with positive results from the phytochemical screening were further quantified.

##### 3.2.1.1 Flavonoid

The protocol for flavonoid characterization was adapted from Kancherla et al. (2019). First, two to three drops of 2N sodium hydroxide were added into 2 mL of the diluted LO extract solution. A color change to yellow would indicate the presence of flavonoids. Two to three drops of 2N hydrochloric acid were subsequently added, returning the color from yellow to colorless, confirming the presence of flavonoids in the extract.

##### 3.2.1.2 Tannin & Phenolic

The protocol for tannin and phenolic characterization was adapted from Kancherla et al. (2019). For this screening, 2 mL of 5% iron (III) chloride (FeCl<sub>3</sub>) was added to 1 mL of the diluted extract solution. A color change from colorless to dark blue/green-black indicates a positive tannin result.

##### 3.2.1.3 Alkaloid

The protocol for alkaloid screening was adapted from Kancherla et al. (2019). In the alkaloid screening, 5 mL of ethanol was added to 2 mL of 2000 ppm LO extract solution, followed by adding 2 mL of Mayer's reagent drop by drop. A positive alkaloid result would result in the formation of a white precipitate.

#### 3.2.1.4 Saponin

The protocol for the saponin screening was adapted from Jayapriya & Shoba (2014). During the saponin screening, 5-8 mL of hot water was added to 2 mL of the diluted LO extract solution, followed by vigorous shaking for at least 10 seconds. After shaking, any bubbles formed were measured. If a foam were present and were higher than 1 cm, the result would confirm the presence of saponin in the extract.

#### 3.2.2 Total Phenolic Content (TPC)

The observation of TPC was conducted in a preliminary study using the same batch of extract. The protocol for quantifying phenolics was adapted from the second edition of Farmakope Herbal of the Indonesian Ministry of Health (2017) and Aryal et al. (2019). Phenolic characterization of the LO extract was conducted utilizing the Folin-Ciocalteu assay. The LO extract (80 mg) was mixed with 10 mL methanol and stirred for 30 minutes. After stirring, the solution was filtered into a 10 mL volumetric flask, and methanol was added until the line.

Furthermore, 2.5 mL of 7.5% Folin-Ciocalteu reagent was added to 500  $\mu$ L of the extract, and the solution was incubated for 8 minutes at room temperature. Then, another 2 mL of 1% sodium hydroxide was added to the solution, followed by another incubation for 1 hour. After incubation, the absorbance was measured using a spectrophotometer (Shimadzu 1280) at a wavelength of 730 nm against the Folin-Ciocalteu reagent as the blank. As a standard, gallic acid was diluted in ethanol in concentrations ranging from 100, 70, 50, 30, 15, and 5  $\mu$ g/mL. The absorbance of the LO bark extract was measured against the gallic acid standard curve, where they will be converted into Gallic Acid Equivalents (GAE) using Equation 3.1. The assay was conducted in triplicate to ensure reliability.

$$GAE: \frac{C \times V}{W \times 1000}$$

**Equation 3.1.** Gallic Acid Equivalent Formula. C: concentration of extract against standard curve (ppm); V: volume of solvent used to dilute the extract; W: mass of extract diluted (g)

#### 3.2.3 Total Flavonoid Content (TFC)

The observation of TFC was conducted in a preliminary study using the same batch of extract. The protocol for quantifying the flavonoids was adapted from the second edition of Farmakope Herbal of the Indonesian Ministry of Health (2017) and Aryal et al. (2019). In TFC characterization, 10 mL of methanol was added to 80 mg of the LO extract and mixed for 30 minutes, followed by filtration. For the observation, 1.5 mL of ethanol, 0.1 mL of 1 M sodium acetate, 0.1 mL of 10% aluminum chloride ( $AlCl_3$ ), and 2.8 mL of type III (distilled) water were added to 500  $\mu$ L of the solution, followed by shaking. After incubation for 30 minutes at room temperature, the absorbance was measured using a spectrophotometer (Shimadzu 1280) at a wavelength of 415 nm against



aluminum chloride as blank. Then, ethanol was added to quercetin as a standard, followed by a serial dilution at 125, 100, 75, 50, and 25 µg/mL concentrations. Finally, the absorbance of the LO bark extract was measured against the quercetin standard curve, where they will be converted into Quercetin Equivalents (QE) using Equation 3.2. The assay was conducted in triplicate to ensure reliability.

$$QE: \frac{C \times V}{W \times 1000}$$

**Equation 3.2.** Quercetin Equivalent Formula. C: concentration of extract against standard curve (ppm); V: volume of solvent used to dilute the extract; W: mass of extract diluted (g)

### 3.2.4 Total Alkaloid Content (TAC)

The observation for TAC was conducted in a preliminary study using the same batch of extract. The protocol used for the alkaloids quantification was adapted from Mythill et al. (2014). Firstly, 50 mg of LO bark extract was diluted in 25 mL of methanol. Next, Bromocresol green (BCG) solution was prepared prior to the quantification by heating 34.9 mg of BCG with 1.5 mL of 2N sodium hydroxide and 2.5 mL type III (distilled) water, followed by dilution to 500 mL with type III water. Finally, a pH 4.7 phosphate buffer solution was prepared by adding citric acid (4.2 grams in 100 mL type III water) to 2 M sodium phosphate (7.16 grams Na<sub>2</sub>HPO<sub>4</sub> in 100 mL type III water).

In order to quantify for alkaloids, 0.5 mL of 2 N HCl was added to 500 µL of extract solution, followed by adding 2.5 mL each of BCG solution and phosphate buffer. The resulting solution was transferred to a separating funnel, where chloroform was added at intervals of 0.5, 1, 1.5, and 2 mL, along with vigorous shaking. Next, the separated chloroform was diluted into 5 mL using chloroform, where the absorbance was measured using a spectrophotometer (Shimadzu 1280) at a wavelength of 470 nm against solutions without the addition of BCG. Then, as a standard, type III (distilled) was added to atropine, followed by a serial dilution at 100, 80, 60, 40, and 20 µg/mL concentrations. The absorbance of the LO bark extract was measured against the atropine standard curve, where they will be converted into Atropine Equivalents (AE) using Equation 3.3. The assay was conducted in triplicate to ensure reliability.

$$AE: \frac{C \times V}{W \times 1000}$$

**Equation 3.3.** Atropine Equivalent Formula. C: concentration of extract against standard curve (ppm); V: volume of solvent used to dilute the extract; W: mass of extract diluted (g)

### 3.2.5 2,2-diphenyl-1-picrylhydrazyl (DPPH) Assay

The protocol for the DPPH assay was adapted from Angjaya (2022). In order to conduct the DPPH assay, 3.9432 mg of DPPH powder was first added to 100 mL methanol to make 0.1 mM DPPH solution. In reaction tubes, 1.5 mL of DPPH solution was then added into 1.5 mL of LO bark extract

serial dilutions at concentrations of 1000, 500, 250, 125, 62.5, 31.25, 15.625, and 7.8125 ppm. As a standard, 1.5 mL of AA at concentrations of 100, 50, 25, 12.5, 6.125, and 3.125 ppm was mixed with 1.5 mL of DPPH solution. As blank, 1.5 mL of DPPH were added to 1.5 mL methanol. The map for the assay could be seen in Figure 3.1. The reaction tubes would then be incubated in the dark at room temperature for 30 minutes. After incubation, 200  $\mu$ L of each samples were pipetted into a 96-well plate as technical replicates, where the absorbances of LO extract and its standard were measured in a plate reader (TECAN Infinite<sup>®</sup>M200 NanoQuant) at a wavelength of 517 nm, measuring the standard curves of AA and LO. The assay was conducted in triplicate to ensure reliability. In order to calculate the free radical scavenging activity, the following equation was used:

$$\text{Free radical scavenging activity (\%)} = \frac{\text{blank} - \text{sample}}{\text{blank}} \times 100\%$$

**Equation 3.4.** Free radical scavenging ability formula

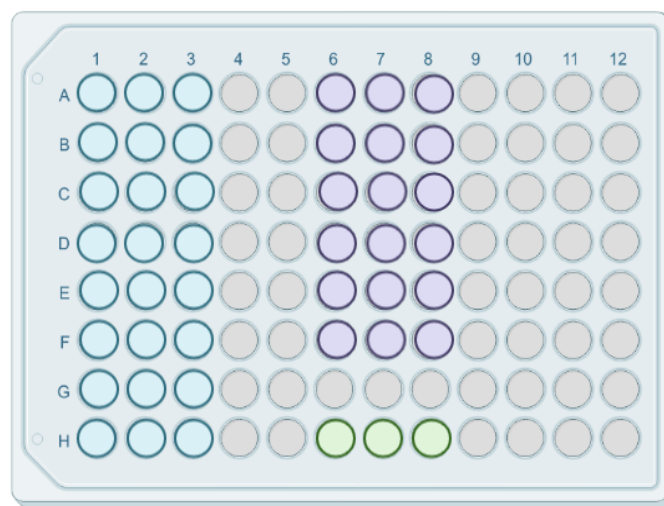


**Figure 3.1.** 96-well plate map for DPPH Assay. The treatments are DPPH + methanol (blank; green), DPPH + LO extract at different ppm (blue), and DPPH + AA at different ppm (purple). Concentration of DPPH + LO from top to bottom: 1000, 500, 250, 125, 62.5, 31.25, 15.625, and 7.8125 ppm; concentration of DPPH + AA from top to bottom: 100, 50, 25, 12.5, 6.125, and 3.125 ppm.

### 3.3 *In vitro* testing in HaCaT cells

The protocol for the cell culture was adapted from Hartrianti et al. (2022).

#### 3.3.1 HaCaT cell culture

The HaCaT cells were obtained from the Indonesia International Institute of Life Sciences (i3L). The cells were thawed and maintained in complete Dulbecco's Modified Eagle Medium (cDMEM), which was Dulbecco's Modified Eagle Medium (DMEM) with 10% Fetal Bovine Serum (FBS)

added. The DMEM is made by dissolving DMEM powder in 500 mL of type 1 water. In addition, 10 mL of penicillin-streptomycin (Pen-Strep) and 3.7 grams of sodium bicarbonate were added to the DMEM solution. The HaCaT cells were then maintained in a CO<sub>2</sub> incubator at 37°C and a CO<sub>2</sub> concentration of 5%. The cells were passaged every 2-3 days to prevent over-confluency.

### 3.3.2 UVB light exposure optimization

UVB light exposure optimization was conducted to identify the suitable time and distance of UVB light exposure that kills around 50% of the seeded cells to be deemed cytotoxic. In the optimization, passaged cells were counted, where  $1 \times 10^4$  of the HaCaT cells from culture were seeded in three wells of a 96-well plate for four replicates, with the addition along with four blanks (media only) and were incubated in the CO<sub>2</sub> incubator at 5% CO<sub>2</sub> and 37°C for 24 hours until confluency of around 90%. The cells were then exposed to UVB in the lamp box (T5 HO 12" Reptisun 15W 5.0 UVB) in the incubator at a distance of 10 and 15 centimeters from the UVB light source and at a time of 3 hours, 6 hours, and 24 hours. As a control, another 96-well plate underwent the identical initial 24-hour incubation and was also incubated for 3 hours, 6 hours, and 24 hours, but not in the lamp box.

The cell viability of the cells was measured after the incubation period by adding 10 µL of 3-[4,5-dimethylthiazol-2-yl]-2,5 diphenyl tetrazolium bromide (MTT) reagent. In order to prevent degradation of the MTT reagent during the treatment, the addition of the MTT reagent was conducted with minimal light exposure. Before the three-hour incubation, the plates were covered with aluminum foil to prevent reagent degradation. The plates were then incubated for three hours at 37°C and a CO<sub>2</sub> concentration of 5%. After incubation, the MTT reaction was stopped using a mixture of isopropanol and hydrochloric acid; the absorbance of the plates were measured using a plate reader (TECAN Infinite®M200 NanoQuant) at a wavelength of 570 nm. Cell viability of the cells were calculated using the following formula:

$$\text{Cell viability (\%)} = \frac{\text{absorbance of sample} - \text{absorbance of blank}}{\text{absorbance of negative control} - \text{absorbance of blank}} \times 100\%$$

**Equation 3.5.** Cell viability formula

The time of incubation and the distance of which the cell viability decreases by 50% was selected for the following cytotoxic and cytoprotective assays.

### 3.3.3 Cytotoxicity assay of *Litsea oppositifolia* extracts and ascorbic acid

Cytotoxicity assay of LO extracts and ascorbic acid was conducted to identify the concentrations of the extracts and its comparator (AA) that kills around 50% of the cells, where cell

viability lower than 50% was deemed cytotoxic. In cytotoxicity assay, passaged HaCaT cells were counted, where  $1 \times 10^4$  cells were seeded into the wells of a 96-well plate, followed by an incubation of 24 hours in the CO<sub>2</sub> incubator at 5% CO<sub>2</sub> and a temperature of 37°C. The cells were then treated with treatments of the LO bark extract and AA as a comparator, as seen in the map in Figure 3.2, and incubated at 5% CO<sub>2</sub> and 37°C. The duration of the treatments followed the best result from the UVB optimization, which was for either 3, 6, or 24 hours.

After the incubation time had passed, an MTT assay was conducted to determine the cell viability through the addition of 10 µL of MTT reagent. In order to prevent degradation of the MTT reagent during the treatment, the addition of the MTT reagent was conducted with minimal light exposure. Before the three-hour incubation, the plates were covered with aluminum foil to prevent reagent degradation. The plates will then be incubated for three hours at 37°C and a CO<sub>2</sub> concentration of 5%. After incubation, the reaction was stopped using a solution of hydrochloric acid and isopropanol, followed by measurement of the absorbance of the plates using a plate reader (TECAN Infinite®M200 NanoQuant) at a wavelength of 570 nm. Cell viability of the cells was calculated using Equation 3.5. If the cell viability is less than 50%, the concentration of said treatment will not be used in the cytoprotective analysis of the LO extract. The assay was conducted in fourplicates to ensure the reliability of the data.

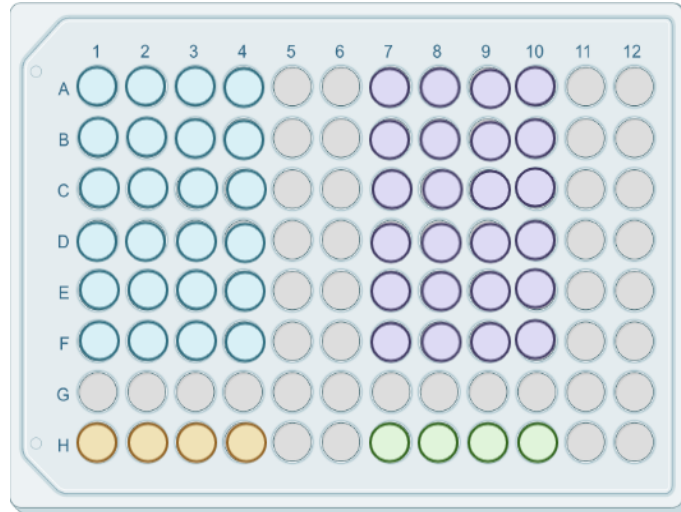


**Figure 3.2** 96-well plate for the cytotoxic assay. The treatments include: cDMEM only (blank; green), cells + cDMEM only (negative control; orange), cells + media + LO extract at different ppm (blue), and cells + media + AA at different ppm (purple). Concentration is decreasing from the top for LO and AA treatments (200, 100, 50, 25, 12.5, 6.25 ppm)

### 3.3.4 Cytoprotective assay

In the cytoprotective assay, seeded HaCaT cells treated with LO bark extract and its comparator (AA) were treated under UVB light irradiation determined from the UVB light

optimization to identify the cytoprotective abilities of the treatments. HaCaT cells were seeded to a 96-well plate with a seeding density of  $1 \times 10^4$  cells, followed by incubation for 24 hours in a CO<sub>2</sub> incubator at 5% CO<sub>2</sub> and a temperature of 37°C. The cells were then treated with the LO bark extract and AA as a comparator at concentrations determined from the cytotoxic assay. The map for the 96-well plate can be seen in Figure 3.3. The plates will undergo UVB radiation in the lamp box at a time and distance predetermined by the UVB irradiation optimization at 5% CO<sub>2</sub> and 37°C. After the incubation at a predetermined time and distance, the cell viability was conducted with an MTT assay, where 10 µL of MTT reagent was used. In order to prevent degradation of the MTT reagent during the treatment, the addition of the MTT reagent was conducted with minimal light exposure. Before the three-hour incubation, the plates were covered with aluminum foil to prevent reagent degradation. The plates were then incubated for three hours at 37°C and a CO<sub>2</sub> concentration of 5%. After incubation, the reaction was first stopped using a mixture of hydrochloric acid and isopropanol; the absorbance of the plates was measured using a plate reader (TECAN Infinite®M200 NanoQuant) at a wavelength of 570 nm. Cell viability of the cells was calculated using Equation 3.5. Results from the cytoprotective assay were compared against the data obtained from the cytotoxic assay. The assay was conducted in fourplicates to ensure the reliability of the data. The data obtained from the research were presented using GraphPad Prism version 9.3.1 as a mean with  $\pm$  standard deviation. Saphiro-Wilk test was used to calculate the normality of the data, followed by a one-way ANOVA and Dunnet's post hoc test. A p-value of less than 0.05 was desired as this result signifies a statistically significant data.

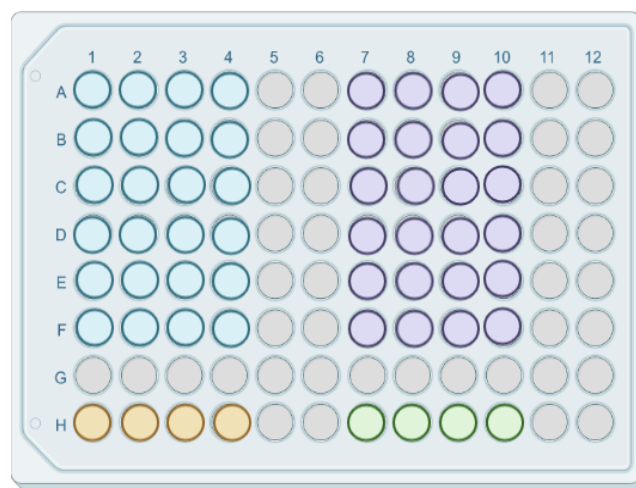


**Figure 3.3.** 96-well plate for the cytoprotective assay. The treatments include: cDMEM only (blank; green), cells + cDMEM only (negative control; orange), cells + media + LO extract at different ppm (blue), and cells + media + AA at different ppm (purple), the concentrations for blue and purple were decided from the cytotoxicity test, where concentrations deemed cytotoxic from the cytotoxic assay were omitted for this analysis.

## CHAPTER 4: RESULTS AND DISCUSSION

### 4.1 *Litsea oppositifolia* bark extract characterization

#### 4.1.1 Phytochemical screening

Phytochemical compounds that were analyzed in this research are flavonoids, phenolics, alkaloids, and saponins. An alkaline reagent test (2N NaOH) was added to the LO extract to detect the presence of flavonoids in the LO bark extract. As the solution turned yellow upon adding 2 N NaOH and back to colorless when added with 2 N HCl, it confirmed the presence of flavonoids in the extract. A color change to yellow results from NaOH breaking the flavonoid bonds to form acetophenone, which is yellow (Fransina et al., 2019).

A ferric chloride test was performed for the qualitative screening of phenolic compounds. After adding 5% iron (III) chloride solution to the extract, a color change to green was observed, thus confirming the presence of phenolics. This color change is attributed to the complex formation between iron chloride (III) and phenols in the extract, which turns the solutions into various colors, including red, green, violet, and blue (Anwar et al., 2019).

In the qualitative screening for alkaloids, Mayer's test was conducted. After adding Mayer's reagent to the extract and ethanol, the presence of alkaloids was confirmed as there was a slight precipitate formation. This result is attributed to forming a potassium-alkaloid complex that could be seen as a precipitate (Parbuntari et al., 2018).

The LO extract solution was shaken vigorously in the qualitative screening for saponin. After 10 minutes, little to no frothing was observed on the solution, which indicates the lack of saponin in the extract. The result of the phytochemical screening is summarized in Table 4.1 below. In addition, because the preliminary results showed the presence of flavonoids, phenolics, and alkaloids, these phytochemicals were screened quantitatively for their exact values.

**Table 4.1.** Phytochemical screening result of LO bark extract. "+" indicates a positive result, while "-" indicates a negative result

Compound	Presence
Flavonoids	+
Phenolics	+
Alkaloids	+
Saponin	-

#### 4.1.2 Total Phenolic Content

Total Phenolic Content (TPC) was conducted to quantify the number of phenolics found in the LO bark extract during the phytochemical screening. The Folin-Ciocalteu assay was used to quantify the total phenolic content in the LO bark extract. The Folin-Ciocalteu test works in a way that the reagent reacts with phenols, forming a molybdenum (V) complex, which is blue in color (Everette et al., 2010). Although the Folin-Ciocalteu test is a rapid and simple method to quantify phenolic compounds, it is non-specific to phenolics (Bibi Sadeer et al., 2020). However, the Folin-Ciocalteu test does not quantify the number of phenolics on its own, but rather its reducing capabilities compared to the comparator, which in this case is gallic acid (Hossain et al., 2011). Therefore, Gallic acid ( $C_6H_2(OH)_3CO_2H$ ) is used as a comparator for the Folin-Ciocalteu test as it is inexpensive, natural, and a stable phenol (Malta & Liu, 2014; Aswar et al., 2021). Besides that, gallic acid is commonly used as a standard for total phenolic content analyses, allowing better comparisons between different data samples (Mu'nisa et al., 2018).

The TPC of the LO bark extract was measured at an absorbance of 730 nm, where the results for TPC quantification were plotted in a graph (Figure 4.1) of absorbance against concentration in parts per million (ppm). The black circle represented the gallic acid standard's absorbance, whereas the blue square represented the absorbance for the LO bark extract. It was determined that the LO bark extract contained  $42.630 \pm 0.682$  mg GAE/g, whereas, in one gram of LO bark extract, there would be the equivalent of 42.630 milligrams of gallic acid in a gram of LO bark extract with a deviation of 0.682 mg.

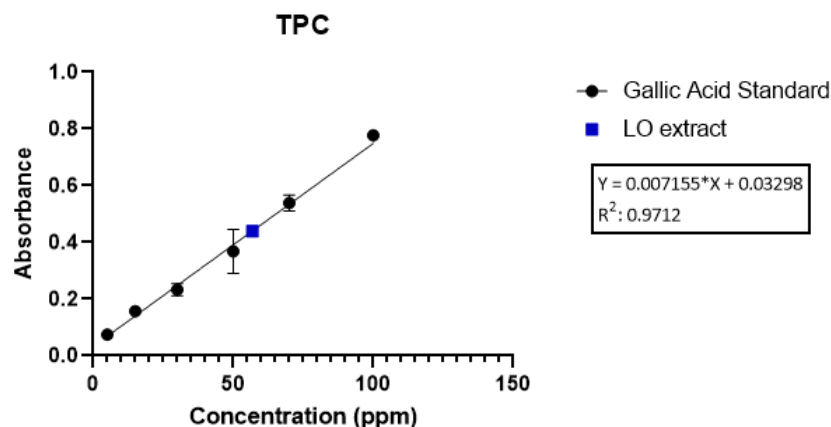


**Figure 4.1.** Total Phenolic Content quantification of LO extract against quercetin as a standard. Black circle: Gallic acid standard curve absorbances; Blue square: LO extract absorbance; Standard curve equation:  $y: 0.007155x + 0.03298$ , R squared value: 0.9712; p-value:  $<0.0001$ .

Compared to a preliminary study by Zakhrifah (2019), the TPC of the LO bark extract is 352.744 mg GAE/g. This is nearly double the phenolics of the extract in n-hexane and six times the amount of gallic acid equivalent in the plant's leaf. The difference in the TPC could be attributed to

the degradation of the extract, as it was exposed to multiple freeze-thaw cycles when it was going to be used, and the sourcing of the plant, as the extract could be obtained from a different source. Comparisons of the phenolic compounds to the same genus, namely *Litsea garciae* and *Litsea cubeba*, were also conducted. Similar to *Litsea oppositifolia*, *Litsea garciae* is also an evergreen plant found in tropical and subtropical regions with various health benefits (Wulandari, Kusuma, & Kuspradini, 2018). *Litsea garciae* that was also macerated contained phenolic content with 40 mg GAE/g in n-hexane and ethyl acetate, along with 90 mg GAE/g in ethanol solution (Wulandari, Kusuma, & Kuspradini, 2018).

#### 4.1.3 Total Flavonoid Content

Total Flavonoid Content was conducted to quantify the flavonoids in the LO bark extract confirmed through the phytochemical screening. In addition, the  $\text{AlCl}_3$  test was conducted to further quantify the number of flavonoids in the extract. The aluminum (III) chloride colorimetric test quantifies flavonoids by the formation of acid stable complexes with the hydroxyl and keto groups of flavones and flavonols and are also capable of forming labile complexes with the A and B ring of flavonoids, which will produce a yellow color (Ahmed & Iqbal, 2018; Pontis et al., 2014). Quercetin ( $\text{C}_{15}\text{H}_{10}\text{O}_7$ ) was used as a standard for the  $\text{AlCl}_3$  as it is highly researched and is abundantly found in plants (Panche et al., 2016). Other than that, quercetin also has keto and hydroxyl groups, which are capable of forming complexes with aluminum (III) chloride and therefore is a strong flavonoid (Masturi et al., 2018).

The TFC of the LO bark extract was measured at an absorbance of 415 nm, where the results obtained from the TFC quantification were plotted in a graph (Figure 4.2) of absorbance against concentration in ppm. The black circle represented the quercetin standard's absorbance, whereas the blue square represented the absorbance for the LO bark extract. The concentration obtained in ppm was then converted into mg QE/g. As a result, it was determined that the LO bark extract contained  $0.993 \pm 0.401$  mg QE/g, where 0.993 milligrams of quercetin as an equivalent with a standard deviation of 0.401 mg would be present in 1 gram of *Litsea oppositifolia* bark extract. However, these results of the flavonoid characterization are significantly lower than those of the same assay being conducted on *Litsea noronhae* blume, as they have a flavonoid content of around 60-70 mg QE/g as opposed to the 0.993 mg QE/g of LO bark extract (Ayu, 2019).



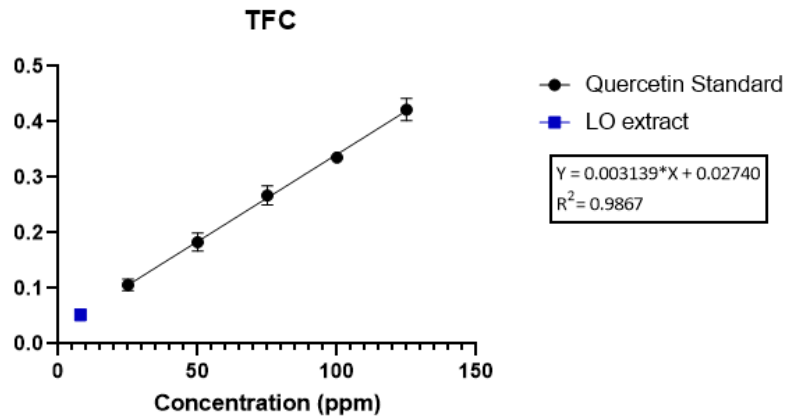


**Figure 4.2.** Total Flavonoid Content quantification of LO extract against quercetin as a standard. Black circle: Quercetin standard curve absorbances; Blue square: LO extract absorbance; Standard curve equation:  $y = 0.003139x + 0.0274$ , R squared value: 0.986; p-value: <0.0001.

#### 4.1.4 Total Alkaloid Content

Total Alkaloid Content was conducted to quantify alkaloids in the *Litsea oppositifolia* bark extract, which was confirmed through the phytochemical screening. In quantifying the alkaloid content, an assay using bromocresol green (BCG) and chloroform. This method was selected as it is a simple, efficient, and sensitive method to quantify the alkaloids in the extract (Fadhil et al., 2007). The mechanism by which this assay works is that the alkaloids form a stable yellow complex with the BCG, which is extractable using chloroform (Fadhil et al., 2007). The compound selected as the standard is atropine ( $C_{17}H_{23}NO_3$ ), as atropine is a natural principal alkaloid that is abundantly found in plants with various uses in the medical field, such as analgesics and sedatives (Jakabová et al., 2012).

The TAC of the LO bark extract was measured at an absorbance of 470 nm, where the results obtained from the TAC quantification were plotted in a graph (Figure 4.3) of absorbance against concentration in ppm. The black circle represented the atropine standard's absorbance, whereas the blue square represented the absorbance for the LO bark extract. The p-value is also less than 0.0001, making the data statistically significant. The concentration obtained in ppm was then converted into mg AE/g. It was determined that the LO bark extract contained  $7.715 \pm 1.414$  mg AE/g, where 0.940 milligrams of atropine as an equivalent with a standard deviation of 1.414 mg would be present in 1 gram of LO bark extract.

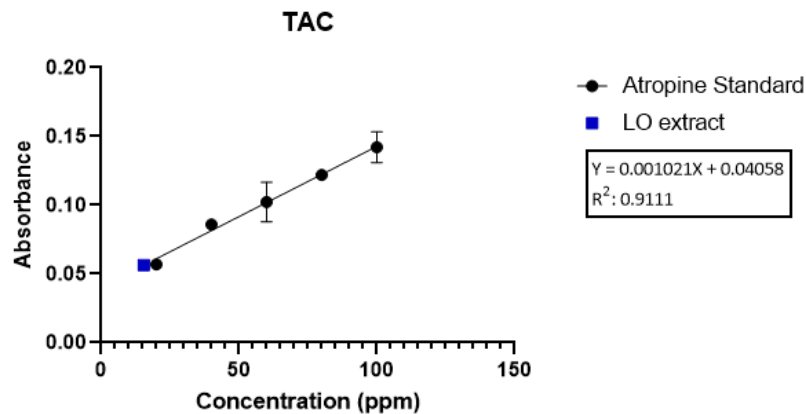


**Figure 4.3.** Total Alkaloid Content quantification of LO extract against quercetin as a standard. Black circle: Atropine standard curve absorbances; Blue square: LO extract absorbance; Standard curve equation:  $y = 0.001021x + 0.04058$ , R squared value: 0.9111; p-value: <0.0001

#### 4.1.5 2,2-diphenyl-1-picrylhydrazyl (DPPH) Assay

The DPPH solution is a stable free radical violet in color at room temperature (Kedare & Singh, 2011; Garcia et al., 2012). DPPH assay relies on the free radical scavenging activity of antioxidants towards the solution, where the free radical in the antioxidants utilizes electron transfer to reduce the nitrogen in the DPPH solution, turning the DPPH solution clear (Garcia et al., 2012; Kedare & Singh, 2011). The presence of antioxidants will reduce the 2,2-diphenyl-1-picrylhydrazyl compound into 1,1-diphenyl-1-picrylhydrazyl (Angjaya, 2022). In the DPPH assay, the lower the half maximal inhibitory concentration ( $IC_{50}$ ), the better the compound's antioxidant activity. This is because of the lower concentration required to scavenge half of the antioxidants in the DPPH solution, where to be considered a good antioxidant, the  $IC_{50}$  has to be lower than 50 ppm (Olugbami et al., 2014; Jadid et al., 2017). The DPPH solution is utilized due to its fast, simple, and highly sensitive properties that could detect weaker antioxidants albeit its sensitivity towards light and ability to react with other radicals (Bibi Sadeer et al., 2020; Garcia et al., 2012).

The solvent used for the DPPH assay is methanol, which was selected as it is more efficient when compared to ethanol and isopropanol (La et al., 2021). As for the standard, ascorbic acid was chosen due to its ability to scavenge free radicals from the aqueous phases of the cells and circulatory system, simulating conditions inside the body (Beyer, 1994). Other than that, other researchers commonly use ascorbic acid, allowing easier comparison, which is a natural and abundant alternative to gallic acid, which could be harmful to humans (Researchgate, 2013).

The results from the DPPH assay were measured in a plate reader at an absorbance of 517 nm. LO bark extract was plotted against AA a graph (Figure 4.4) of percent (%) inhibition against concentration in ppm. The blue circle represented LO extract, whereas the black square represented AA. From the graph, it was observed that the  $IC_{50}$  of the LO extract is  $48.660 \text{ ppm} \pm 3.97$ , whereas the

IC<sub>50</sub> of AA was observed at 3.853 ppm ± 2.27. Based on these results, it could be concluded that ascorbic acid had stronger antioxidant activity in comparison to *Litsea oppositifolia* bark extract.

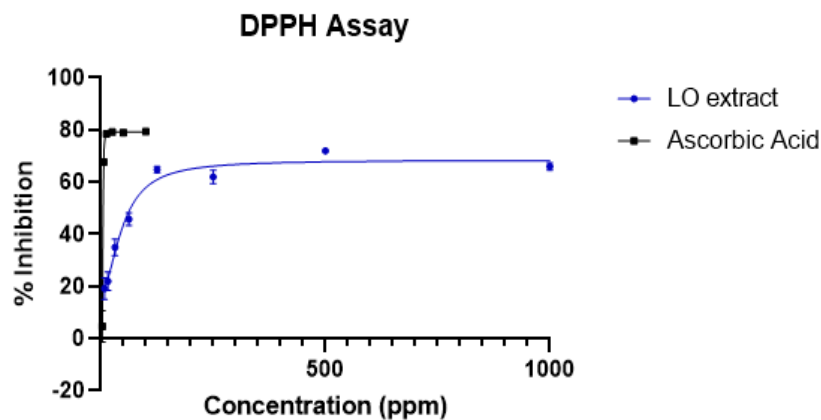


**Figure 4.4.** DPPH assay results of LO bark extract (blue) and Ascorbic acid (black). R squared value LO extract: 0.9660; R squared value Ascorbic Acid: 0.9946.

Although the IC<sub>50</sub> of the LO bark extract is considered strong, it is still higher than that of the LO bark extract in ethanol conducted in a preliminary study by Zakhrifah (2019), where the IC<sub>50</sub> of the extract was 8.31 ± 0.04 ppm. Zakhrifah (2019) also showed that LO bark extract in ethanol had the highest antioxidant activity compared to other solvents and parts of the plant, such as ethyl acetate and n-hexane, and the leaf of the plant instead of the bark. As mentioned previously, a higher IC<sub>50</sub> signified a weaker antioxidant activity. The difference in the IC<sub>50</sub> of these extracts could be attributed to the extract degradation, as the extracts were stored in the freezer prior to usage, and the plant source of the extracts might be different. When compared to other species of the same genus, namely *Litsea cubeba* and *Litsea angulata*, LO bark extract had stronger antioxidant activity, where their bark macerated in ethanol showed an IC<sub>50</sub> of 19.26 ppm and 26.81 ppm, respectively (Wulandari et al., 2018; Kuspradini et al., 2019).

## 4.2 *In vitro* assay in HaCaT cell

### 4.2.1 UVB light irradiation optimization

The time for optimizing the UVB irradiation towards the HaCaT cells was 3, 6, and 24 hours at a distance of 10 and 15 centimeters from the light source. This time was chosen as the time UV radiation is strongest during the day is between 10 am and 4 pm, which is for 6 hours (EPA, 2022). The consideration for 3 hours was that the duration is half of the strongest UV radiation, whereas, for 24 hours, it is an attempt to ensure cell death. The effect of UVB light irradiation on HaCaT cells was analyzed by exposing the seeded HaCaT cells with a density of 1×10<sup>4</sup> cells to UVB light at distances of

10 and 15 centimeters from the light source and at a time of 3, 6, and 24 hours. After exposure towards the designated time and distance, the cell viability was assessed using a 3-(4,5-dimethylthiazol-2-yl)-2,5-diphenyltetrazolium (MTT) assay. MTT assay (seen in Figure 4.5) is a colorimetric assay that utilizes the NADPH from cellular respiration in the mitochondria to reduce the tetrazolium dye in the MTT reagent into formazan crystals, which are purple (Kuetze et al., 2017).

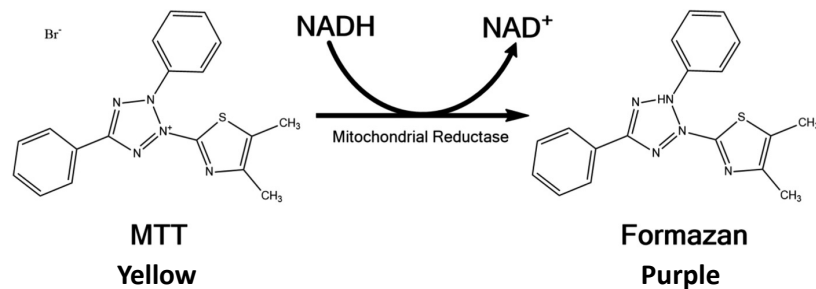


**Figure 4.5.** MTT Assay mechanism (Kamiloglu et al., 2020)

However, this only works in viable cells; therefore, the formazan formed is proportional to the viability of the cells (Wachsmann & Lamprecht, 2012). The formazan has to be solubilized using organic solvents to a colored solution, where the absorbance would be measured at 570 nm (Kuetze et al., 2017).

The results for UVB irradiation on HaCaT cells for the time of 3 hours are seen in Figure 4.6 below, where the graph is plotted as cell viability (%) of the HaCaT cells against the different types of treatment. The treated cells at a distance of 10 cm and 15 cm showed a cell viability of  $73.49\% \pm 24.97$  and  $69.75\% \pm 20.69$ , respectively.

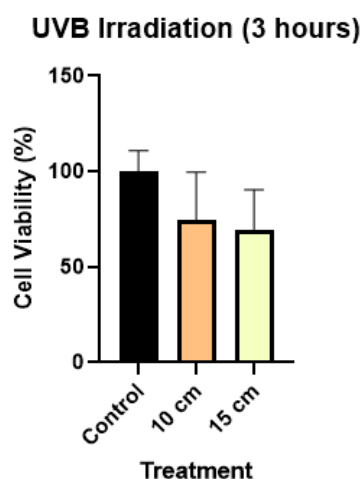


**Figure 4.6.** UVB Irradiation optimization of HaCaT cells at 3 hours. The data is presented as mean  $\pm$  standard deviation. Black: Control (did not undergo UV irradiation); Orange: Underwent UV irradiation from a distance of 10 cm. Yellow: Underwent UV irradiation from a distance of 15 cm.

The results of UVB irradiation towards HaCaT cells at a time of 6 hours are seen in Figure 4.6 below, where the graph is plotted as cell viability (%) of the HaCaT cells against the different types of treatment. The cells exposed at a distance of 10 cm showed a cell viability of  $54.13\% \pm 9.47$ , while the treated cells at a distance of 15 cm showed a cell viability of  $49.81\% \pm 7.64$ .

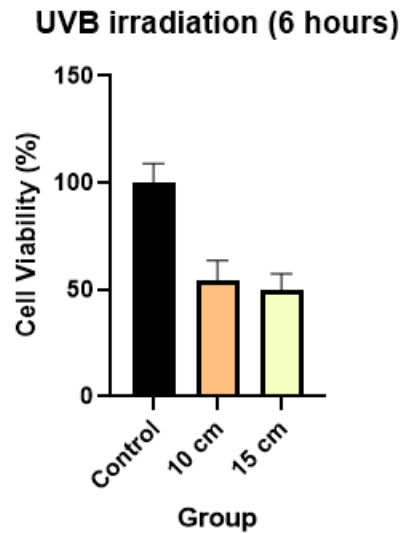


**Figure 4.7.** UVB Irradiation optimization of HaCaT cells at 6 hours. The data is presented as mean  $\pm$  standard deviation. Black: Control (did not undergo UV irradiation); Orange: Underwent UV irradiation from a distance of 10 cm. Yellow: Underwent UV irradiation from a distance of 15 cm.

Lastly, UVB irradiation was done on the HaCaT cells at 24 hours, as seen in Figure 4.7, where the graph is plotted as cell viability (%) of the HaCaT cells against the different types of treatment. The control for the 24-hour optimization showed a cell viability of  $100\% \pm 13.25$ . Against the control cells, the treated cells at a distance of 10 cm showed a cell viability of  $19\% \pm 9.19$ , whereas the treated cells at a distance of 15 cm showed a cell viability of  $10.35\% \pm 2.52$ .

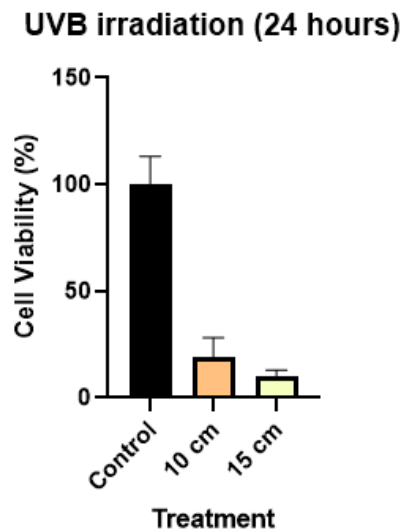


**Figure 4.8.** UVB Irradiation optimization of HaCaT cells at 24 hours. The data is presented as mean  $\pm$  standard deviation. Black: Control (did not undergo UV irradiation); Orange: Underwent UV irradiation from a distance of 10 cm. Yellow: Underwent UV irradiation from a distance of 15 cm.

The results from the UV irradiation optimization showed that exposure of the HaCaT cells to the UVB light is indeed cytotoxic to the cells, as the cell viability decreased even in the shortest amount of exposure. The adverse effects of UVB irradiation could be seen, where the UVB light causes damage to the HaCaT cells by inducing ROS formation that causes oxidative stresses that may result in melanoma (Han et al., 2021). This is further supported by excessive ROS formation in the skin allowing the keratinocytes to enter apoptosis (Dutordoir & Bates, 2016). Excessive UV exposure also promotes cytokine secretion that induces inflammation that could lead to hyperkeratosis, thickened *stratum corneum*, the outermost layer of the epidermis (Kim et al., 2013; D'Orazio et al., 2013; Farci & Mahabal, 2022). HaCaT cells exposed to UVB exposure by Kim et al. (2013) also showed that the cell viability of the cells decreases as UVB irradiation increases. These cells were selected as the skin model as it stimulates keratinocytes, which are most abundantly present in the epidermis of the skin, where the UVB radiation penetrates, as it does until the *stratum basale*, which is the innermost part of the epidermis (Yousef et al., 2021; Wang et al., 2019; Han et al., 2021).

As the UVB irradiation optimization at 3 hours yielded a high standard deviation, and the optimization at 24 hours was too cytotoxic for the cells, UVB irradiation for 6 hours was chosen for the subsequent cytotoxic and cytoprotective assays. For the cytoprotective assay, irradiation from a distance of 15 cm will be chosen due to its cell viability under 50% and a lower standard deviation compared to irradiation from a distance of 10 cm.

#### 4.2.2 Cytotoxic assay

The cytotoxic assay was conducted to assess the toxicity of a test compound, the *Litsea oppositifolia* bark extract, and its comparator ascorbic acid against the cells, which in this case is HaCaT, by measuring its cell viability after exposure to the test compound (Riss et al., 2019). A substance would be considered cytotoxic if, after exposure to the substance, the cell viability of the treated cells was reduced by 50% (Ogbole et al., 2017). Ascorbic acid was chosen as the comparator for the cytotoxicity assay as it has been confirmed to suppress ROS generation in cell culture experiments (Wu et al., 2020).

Cytotoxic assay of the *Litsea oppositifolia* bark extract and ascorbic acid was conducted in a time of 6 hours, following the results from the UVB light irradiation optimization test. Seeded cells to a density of  $1 \times 10^4$  were first incubated for 24 hours until confluent before adding LO bark extract and AA treatments, as seen on the map in Figure 3.2. Next, the treated cells were incubated for 6 hours before washing and adding MTT reagent for the assay. The cells were then incubated for another three hours before adding stop solution and assessing the cell viability through the plate reader at a wavelength of 570 nm.

The cytotoxic assay results of *Litsea oppositifolia* bark extract can be seen in Figure 4.8, where the graph is plotted as cell viability (%) of HaCaT cells against the concentration of LO bark extract in ppm. The graph was plotted as mean  $\pm$  standard deviation. Based on the graph, it could be observed that the cell viabilities of the HaCaT cells in the range of LO bark extract concentrations are more than or almost equal to 100%, albeit the high standard deviations. Because of this, it could be concluded that the extract is not cytotoxic toward the HaCaT cells up to the 200 ppm concentration, and all concentrations will be used in the cytoprotective assay. One-way ANOVA was performed on the graph after passing the normality test, but no significant difference was observed from the control.

### Cytotoxic Assay of LO Bark Extract

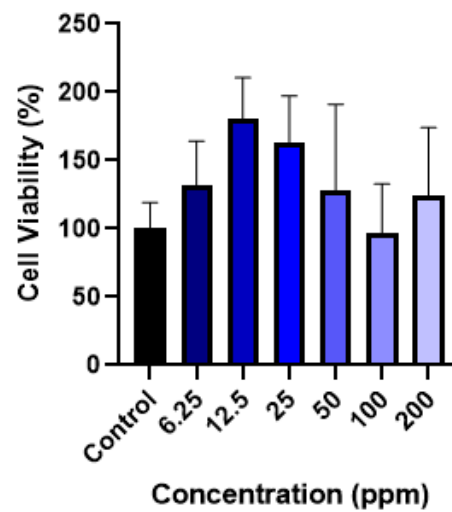


**Figure 4.9.** Cell viability of HaCaT cells when treated with LO bark extract after 6 hours of incubation. The data is presented as mean  $\pm$  standard deviation. Black: negative control (cells with no treatment); Concentrations of LO bark extract is increasing from dark blue to light blue.

On the other hand, the cytotoxicity results of ascorbic acid can be seen in Figure 4.9, where the graph is plotted as cell viability (%) of HaCaT cells against the concentration of AA in ppm. The graph was presented as mean  $\pm$  standard deviation. Based on the graph, it could be observed that the cell viability of the HaCaT cells started to decrease significantly at 50 ppm of ascorbic acid, indicating that the ascorbic acid starts to be cytotoxic towards the cells at 50 ppm. The decrease in cell viability might be attributed to the generation of extracellular  $H_2O_2$  as the mechanism of ascorbic acid (Fröhberg et al., 2020; Wu et al., 2020). Because of this, the ascorbic acid concentrations used in the cytoprotective analysis would only be up to 50 ppm. One-way ANOVA was performed after passing the normality test, but no significant difference was observed from the control. A high standard deviation was observed from the LO bark extract and AA testing, which could be attributed to pipetting errors throughout the experiment and uneven distribution of the seeding density of the cells.



### Cytotoxic Assay of Ascorbic Acid

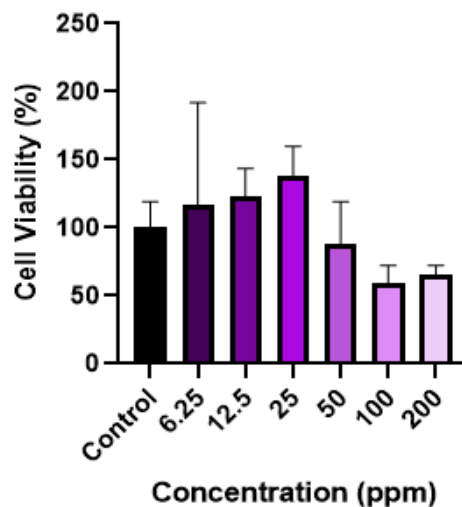


**Figure 4.10.** Cell viability of HaCaT cells when treated with ascorbic acid after 6 hours of incubation. The data is presented as mean  $\pm$  standard deviation. Black: negative control (cells with no treatment); Concentrations of ascorbic acid are increasing from dark purple to light purple.

#### 4.2.3 Cytoprotective assay

The cytoprotective assay was conducted to assess the ability of the LO bark extract and AA to protect the cells against UVB radiation. Cytoprotective assay of the *Litsea oppositifolia* bark extract and ascorbic acid was conducted in 6 hours and from a distance of 15 cm from the UVB light source following the results from the UVB light irradiation optimization test. Seeded cells to a density of  $1 \times 10^4$  were first incubated for 24 hours until confluent before adding LO bark extract and AA treatments, as seen on the map in Figure 3.3, omitting the wells for ascorbic acid at 100 and 200 ppm. The treated cells were then incubated for 6 hours and at a distance of 15 cm from the UVB lamp before washing and adding MTT reagent for the assay. The cells were then incubated for another three hours before adding stop solution and assessing the cell viability through the plate reader at a wavelength of 570 nm.

The result for the cytoprotective assay could be seen in Figure 4.10, where the graph is plotted as HaCaT cell viability (%) against concentration in ppm. The graph was presented as mean  $\pm$  standard deviation. Based on the graph, all concentrations of the LO bark extract showed a cytoprotective effect compared to the untreated cell, with a significant protective effect at 100 ppm of LO bark extract. This is due to the higher cell viability of all treatments above the 0 ppm treatment, and the statistical significance of  $P < 0.05$  when one way ANOVA was conducted, after passing the normality test. These results showed that LO bark extract indeed had cytoprotective effects towards UVB irradiation.

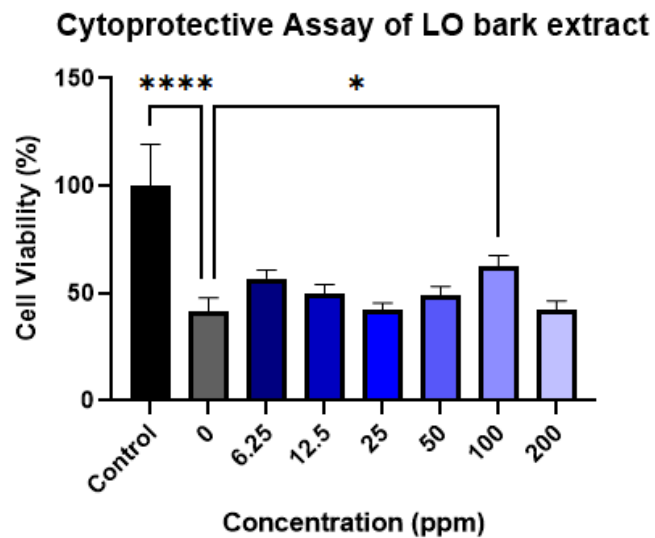


**Figure 4.11.** Cytoprotective assay results of LO bark extract after six hours of UVB incubation time from a distance of 15 cm towards HaCaT cells. The data is presented as mean  $\pm$  standard deviation. Black: negative control (did not enter UV box); Grey: untreated cells irradiated with UV. Concentrations of LO bark extract is increasing from dark blue to light blue. \* indicates statistical significant difference against the negative control ( $P < 0.05$ ). \*\*\*\* indicates a statistical significant difference against the negative control ( $P < 0.0001$ ).

On the other hand, the cytoprotective results of ascorbic acid can be seen in Figure 4.11, where the graph is plotted as cell viability (%) of HaCaT cells against the concentration of AA in ppm. The graph was presented as mean  $\pm$  standard deviation. Based on the graph, it could be observed that the cell viability of the treated HaCaT cells showed a significant cytoprotective effect at concentrations of 25 ppm and 50 ppm. This could be attributed to the increased cell viability when compared to the 0 ppm treatment, and when one way ANOVA was conducted after the normality test had passed, a statistical significance of  $P < 0.01$  and  $P < 0.05$  were observed at AA treatments of 25 and 50 ppm respectively. The decrease in statistical significance between ascorbic acid treatments at concentrations of 25 ppm and 50 ppm could be attributed to the the generation of extracellular  $H_2O_2$  as the mechanism of ascorbic acid, as observed in the cytotoxic assay of ascorbic acid (Fröhberg et al., 2020; Wu et al., 2020). The results would signify that ascorbic acid had better cytoprotective ability when compared to LO bark extract, as a lower concentration was required to reach a significant cytoprotective effect.

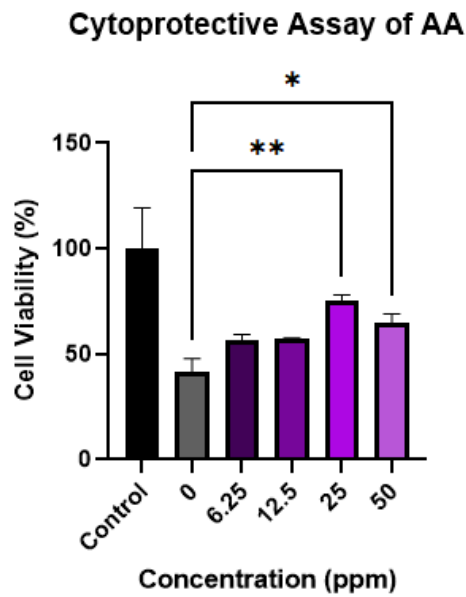


**Figure 4.12.** Cytoprotective assay results of ascorbic acid after six hours of UVB incubation time from a distance of 15 cm towards HaCaT cells. The data is presented as mean  $\pm$  standard deviation. Black: negative control (did not enter UV box); Grey: untreated cells irradiated with UV. Concentrations of ascorbic acid are increasing from dark purple to light purple.

\* indicates statistical significant difference against the negative control ( $P < 0.05$ ). \*\* indicates a statistical significant difference against the negative control ( $P < 0.01$ ).

Results from the cytoprotective assay were supported by the DPPH assay, as ascorbic acid had a significantly lower  $IC_{50}$  when compared to LO bark extract, which indicated that ascorbic acid was still a stronger antioxidant when compared to LO bark extract. However, results from the DPPH assay confirmed that both are strong antioxidants, as the  $IC_{50}$  of both treatments is less than 50 ppm, which is eligible to be considered a strong antioxidant. In addition, results from quantifying phenolics, flavonoids, and alkaloids also confirmed the presence of such phytochemicals in different amounts, which further supports the antioxidant properties of LO bark extract.

## CHAPTER 5: CONCLUSION AND RECOMMENDATIONS

*Litsea oppositifolia* bark extract was measured for its cytoprotective ability against UVB exposure due to its antioxidant properties, which is also present in other *Litsea* plants. This research combined the preliminary results of TPC, TAC, TFC, and phytochemical screening of the extract, also with evaluation of the antioxidant content through DPPH assay, followed with cytotoxic and cytoprotective assay towards HaCaT cells after optimization of the UVB exposure. Although the DPPH assay showed that LO bark extract is a strong antioxidant with an  $IC_{50}$  of  $48.660 \text{ ppm} \pm 3.97$ , it is still weaker than ascorbic acid with an  $IC_{50}$  of  $3.853 \text{ ppm} \pm 2.27$ .

Prior to the cytotoxic and cytoprotective assays of the LO bark extract, UVB optimization was carried out, where the optimum time and distance that kills roughly 50% of the HaCaT cells were determined at 6 hours from a distance of 15 cm. Cytotoxicity assay for LO bark extract showed no cytotoxic activity, whereas for AA, the decrease in cell viability at 50 ppm was determined to be cytotoxic and therefore the concentration of AA at 100 and 200 ppm were not used for the cytoprotective assay. The cytoprotective assay showed that LO bark extract exhibited cytoprotective abilities at 100 ppm when exposed to UVB light. However, AA still had stronger cytoprotective abilities at lower concentrations, namely 25 and 50 ppm. Therefore, although it was confirmed that LO bark extract exhibited antioxidant activity and cytoprotective abilities, it is still inferior when compared to AA.

For further research, fresh extract should be made to ensure no degradation occurred prior to the experiment, followed by improvement of aseptic techniques and laboratory skills to prevent contamination and unwanted errors. Comparing the extraction method and solvent used for obtaining the LO bark extract for its phytochemical may also be a viable option. Identifying the compounds that might be contained in the extract that could exert protective abilities against UV radiation could also be attempted using LC-MS. A major limitation in this research is the lack of study of the effects of the LO bark extract towards the gene expression of the cells, therefore gene expression analyses could be conducted to further investigate the effects of LO bark extract towards the cells.

## REFERENCES

- Adiyanto, S. A. (2022). *In vitro cytoprotective activity study of cocoa pod husk (Theobroma cacao L.) extract against blue light*. (Thesis, Indonesia International Institute of Life Sciences, Jakarta, Indonesia).
- Ahmed, F., & Iqbal, M. (2018). Antioxidant activity of *Ricinus communis*. *Organic & Medicinal Chem IJ*, 5(4).
- Anwar, M. S., Uppal, S., Ganguly, G., Chitkara, A., Bhardwaj, G. N., Kumar, S., & Wadhwa, N. (2019). Chemistry textbook for class XII. *National council of educational research and training*. ISBN: 81-7450-648-9
- Aswar, Malik, A., Hamidu, L., Najib, A. (2021). Determination of total phenolic content of nyirih stem bark extract (*xylocarpus granatum* J koeing) using UV-vis spectrophotometry method. *Jurnal Fitofarmaka Indonesia*, 8(3).
- Aryal, S., Baniya, M. K., Danekhu, K., Kunwar, P., Gurung, R., & Koirala, N. (2019). Total phenolic content, flavonoid content and antioxidant potential of wild vegetables from western nepal. *Plants (Basel, Switzerland)*, 8(4), 96.
- Ayu, M. P. (2019). *Uji aktivitas antioksidan dan penapisan fitokimia dari ekstrak daun dan kulit batang medang putih (Litsea noronhae Blume)*. (Thesis, University of Indonesia, Depok, Indonesia).
- Basheer, S. M., Chellappan, S., & Sabu, A. (2022). Chapter 8- Enzymes in fruit and vegetable processing. *Value-addition in food products and processing through enzyme technology*, 101-110. Academic Press.
- Beckhauser, T. F., Francis-Oliveira, J., & De Pasquale, R. (2016). Reactive Oxygen Species: physiological and physiopathological effects on synaptic plasticity. *Journal of experimental neuroscience*, 10(Suppl 1), 23–48.
- Bernstein, E. F., Sarkas, H. W., & Boland, P. (2021). Iron oxides in novel skin care formulations attenuate blue light for enhanced protection against skin damage. *Journal of Cosmetic Dermatology*, 20(2), 532-537.
- Beyer, R. E. (1994). The role of ascorbate in antioxidant protection of biomembranes: Interaction with vitamin E and coenzyme Q. *Journal of Bioenergetics and Biomembranes*, 26.
- Bibi Sadeer, N., Montesano, D., Albrizio, S., Zengin, G., & Mahomoodally, M. F. (2020). The versatility of antioxidant assays in food science and safety—chemistry, applications, strengths, and limitations. *Antioxidants*, 9(8), 709.
- Chriscensia, E. (2022). *In vitro cytoprotective studies of Theobroma cacao L. pod husk extract against pollution models*. (Thesis, Indonesia International Institute of Life Sciences, Jakarta, Indonesia)
- Chung, K. T., Wong, T. Y., Wei, C. I., Huang, Y. W., & Lin, Y. (1998). Tannins and human health: a review. *Critical reviews in food science and nutrition*, 38(6), 421–464.
- Coats, J. G., Maktabi, B., Abou-Dahech, M. S., & Baki, G. (2020). Blue light protection, Part I—Effects of blue light on the skin. *Journal of Cosmetic Dermatology*.
- Colombo, I., Sangiovanni, E., Maggio, R., Mattozzi, C., Zava, S., Corbett, Y., Fumagalli, M., Carlino, C., Corsetto, P. A., Scaccabarozzi, D., Calvieri, S., Gismondi, A., Taramelli, D., & Dell'Agli, M. (2017). HaCaT Cells as a reliable in vitro differentiation model to dissect the inflammatory/repair response of human keratinocytes. *Mediators of inflammation*, 2017, 7435621.
- Dalimunthe, A., Hasibuan, P. A. Z., Silalahi, J., & Satria, D. (2018). Antioxidant activity of alkaloid fractions of *Litsea cubeba* lour fruits. *Asia Journal of Pharmaceutical and Clinical Research*.
- Dalimunthe, A., Pertiwi, D., Muhammad, M., Satria, D. (2021). Analysis of antioxidant activity, total phenolic and flavonoid contents of ethanol extract of *Litsea cubeba* Lour. Bark. *E3S Web of Conferences*, 332.

- Dey, P., Kundu, A., Kumar, A., Gupta, M., Lee, B. M., Bhakta, T., Dash, S., & Kim, H. S. (2020). Analysis of alkaloids (indole alkaloids, isoquinoline alkaloids, tropane alkaloids). *Recent Advances in Natural Products Analysis*, 505–567.
- D'Orazio, J., Jarrett, S., Amaro-Ortiz, A., & Scott, T. (2013). UV radiation and the skin. *International journal of molecular sciences*, 14(6), 12222–12248.
- EPA. (n.d.). Ultraviolet (UV) Radiation and Sun Exposure [Internet]. Retrieved on 13 September 2022 from <https://www.epa.gov/radtown/ultraviolet-uv-radiation-and-sun-exposure>
- Everette, J. D., Bryant, Q. M., Green, A. M., Abbey, Y. A., Wangila, G. W., & Walker, R. B. (2010). Thorough study of reactivity of various compound classes toward the Folin-Ciocalteu reagent. *Journal of agricultural and food chemistry*, 58(14), 8139–8144.
- Fadhi, S., Reza, M. H., Rouhollah, G., & Reza, V. R. M. (2007). Spectrophotometric determination of total alkaloids in *Peganum harmala* L. using bromoscerol green. *Research Journal of Phytochemistry*
- Farci, F., & Mahabal, G. D. (2022). *Hyperkeratosis [StatPearls]*. Retrieved on 18 December 2022 from <https://www.ncbi.nlm.nih.gov/books/NBK562206/>
- Fernández-García, E. (2014). Skin protection against UV light by dietary antioxidants. *Food & Function*, 5(9), 1994.
- Ferreira M. U. (2022). Alkaloids in future drug discovery. *Molecules (Basel, Switzerland)*, 27(4), 1347.
- Forest Research Institute Malaysia. (2005). Taxonomic notes on Bornean *Litsea*, *Lindera*, *Neolitsea* and *Iteadaphne* (Lauraceae). *Gardens' Bulletin Singapore*, 57, 217-246.
- Fransina, E. G., Tanasale, M. F. J. D. P., Latupeirissa, J., Malle, D., & Tahapary, R. (2019). Phytochemical screening of water extract of gayam (*Inocarpus edulis*) bark and its amylase inhibitor activity assay. *IOP conference series: Materials Science and Engineering (509)*.
- Frömberg, A., Gutsch, D., Schulze, D., Vollbracht, C., Weiss, G., Czubyko, F., & Aigner, A. (2011). Ascorbate exerts anti-proliferative effects through cell cycle inhibition and sensitizes tumor cells towards cytostatic drugs. *Cancer chemotherapy and pharmacology*, 67(5), 1157–1166.
- Gallagher, R. P., Lee, T. K., Bajdik, C. D., & Borugian, M. (2010). Ultraviolet radiation. *Chronic dis*
- Garcia, E. J., Oldoni, T. L. C., de Alencar, S. M., Reis, A., Loguercui, A. D., & Grande, R. M. H. (2012). Antioxidant activity by DPPH assay of potential solutions to be applied on bleached teeth. *Braz. Dent. J*, 23(1).
- Global Biodiversity Information Facility. (2017). *Litsea oppositifolia* Gibbs in GBIF Secretariat. Retrieved 20 January 2023 from <https://www.gbif.org/species/4181852>
- Han, E. J., Kim, S. Y., Han, H. J., Kim, H. S., Kim, K. N., Fernando, I. P. S., Madusanka, D. M. D., Dias, M. K. H. M., Cheong, S. H., Park, S. R., Han, Y. S., Lee, K., & Ahn, G. (2021). UVB protective effects of *Sargassum horneri* through the regulation of Nrf2 mediated antioxidant mechanism. *Scientific reports*, 11.
- Hartrianti, P. D., Sutejo, R., Gustiananda, M., Wibowo, E. C., & Adiyanto, S. A. (2022). Protocol: in vitro cytoprotective study against blue light exposure. *i3L Press*.
- Heinrich, M., Mah, J., & Amirkia, V. (2021). Alkaloids Used as Medicines: Structural phytochemistry meets biodiversity-an update and forward look. *Molecules (Basel, Switzerland)*, 26(7), 1836.
- Hossain, M. A., Shah, M. D., Gnanaraj, C., & Iqbal, M. (2011). In vitro total phenolics, flavonoids contents and antioxidant activity of essential oil, various organic extracts from the leaves of tropical medicinal plant *Tetrastigma* from Sabah. *Asian Pacific Journal of Tropical Medicine*, 4(9), 717–721.
- Jakabová, S., Vincze, L., Farkas, Á., Kilár, F., Boros, B., & Felinger, A. (2012). Determination of tropane alkaloids atropine and scopolamine by liquid chromatography–mass spectrometry in plant organs of *Datura* species. *Journal of Chromatography A*, 1232, 295–301.
- Jayapriya, G., & Shoba, F. G. (2014). Screening for phytochemical activity of *Urechites lutea* plant. *Asian Journal of Plant Science and Research*, 4(6), 20-24.
- Juzeniene, A., & Moan, J. (2012). Beneficial effects of UV radiation other than via vitamin D production. *Dermato-endocrinology*, 4(2), 109–117.

- Kamle, M., Mahato, D. K., Lee, K. E., Bajpai, V. K., Gajurel, P. R., Gu, K. S., & Kumar, P. (2019). Ethnopharmacological Properties and Medicinal Uses of *Litsea cubeba*. *Plants (Basel, Switzerland)*, 8(6), 150. <https://doi.org/10.3390/plants8060150>
- Kamiloglu, S., Sari, G., Ozdal, T., & Capanoglu, E. (2020). Guidelines for cell viability assays. *Food Frontiers*, 1: 332–349.
- Kancherla, N., Dhakshinamoothi, A., Chitra, K., & Komaram, R. B. (2019). Preliminary analysis of phytoconstituents and evaluation of anthelmintic property of *Cayratia auriculata* (In Vitro). *Maedica*, 14(4), 350–356.
- Karapetsas, A., Voulgaridou, G. P., Iliadi, D., Tsochantaridis, I., Michail, P., Kynigopoulos, S., Lambropoulou, M., Stavropoulou, M. I., Stathopoulou, K., Karabournioti, S., Aligiannis, N., Gardikis, K., Galanis, A., Panayiotidis, M. I., & Pappa, A. (2020). Honey extracts exhibit cytoprotective properties against UVB-induced photodamage in human experimental skin models. *Antioxidants*, 9(7), 566.
- Kedare, S. B., & Singh, R. P. (2011). Genesis and development of DPPH method of antioxidant assay. *Journal of food science and technology*, 48(4), 412–422.
- Kementerian Kesehatan RI. (2017). *Farmakope Herbal Indonesia Edisi II*. Jakarta: Kementerian Kesehatan RI.
- Kim, S. B., Kang, O. H., Joung, D. K., Mun, S. H., Seo, Y. S., Cha, M. R. Y., S. Y., Shin, D. W., & Kwon, D. Y. (2013). Anti-inflammatory effects of tectroside on UVB-induced HaCaT cells. *International Journal of Molecular Medicine*.
- Kong, D.-G., Zhao, Y., Li, G.-H., Chen, B.-J., Wang, X.-N., Zhou, H.-L., ... Shen, T. (2015). The genus *Litsea* in traditional Chinese medicine: An ethnomedical, phytochemical and pharmacological review. *Journal of Ethnopharmacology*, 164, 256–264.
- Kuete, V., Karaosmanoğlu, O., & Sivas, H. (2017). *Anticancer Activities of African Medicinal Spices and Vegetables. Medicinal Spices and Vegetables from Africa*, 271–297. doi:10.1016/b978-0-12-809286-6.00010-8
- Kumar, S., & Pandey, A. K. (2013). Chemistry and biological activities of flavonoids: an overview. *TheScientificWorldJournal*, 2013, 162750.
- Kupina, S., Fields, C., Roman, M. C., & Brunelle, S. L. (2018). Determination of Total Phenolic Content using the Folin-C Assay: Single-Laboratory Validation, First Action 2017.13. *Journal of AOAC International*, 101(5), 1466–1472.
- Kuspradini, H., Wulandari, I., Putri, A. S., Tiya, S. Y., & Kusuma, I. W. (2019). *Phytochemical, antioxidant and antimicrobial properties of Litsea angulata extracts. F1000Research*, 7, 1839.
- Kurek, J. (2019). Introductory chapter: Alkaloids - their importance in nature and for human life. In (Ed.), alkaloids - their importance in nature and human life. *IntechOpen*.
- La, J., Kim, M. J., & Lee, J. (2021). Evaluation of solvent effects on the DPPH reactivity for determining the antioxidant activity in oil matrix. *Food science and biotechnology*, 30(3), 367–375.
- Liang, N., & Kitts, D. D. (2014). Antioxidant property of coffee compounds: assessment of methods that define mechanisms of action. *Molecules*.
- Lin, D., Xiao, M., Zhao, J., Li, Z., Xing, B., Li, X., Kong, M., Li, L., Zhang, Q., Liu, Y., Chen, H., Qin, W., Wu, H., & Chen, S. (2016). An overview of plant phenolic compounds and their importance in human nutrition and management of type 2 diabetes. *Molecules (Basel, Switzerland)*, 21(10), 1374.
- Malta, L. G., & Liu, R. H. (2014). Analyses of total phenolics, total flavonoids, and total antioxidant activities in foods and dietary supplements. *Reference Module in Food Science*
- Masturi, Alighiri, D., Nuzulina, K., Rodhiyah, M., & Drastisianti, A. (2019). Optimization of condition extraction in quantification of total flavonoid content in the seeds of the *Arummnais (Magnifera indica L.)* mango from Indonesia. *Journal of Physics: Conference Series*.

- Moses, T., Papadopoulou, K. K., & Osbourn, A. (2014). Metabolic and functional diversity of saponins, biosynthetic intermediates and semi-synthetic derivatives. *Critical reviews in biochemistry and molecular biology*, 49(6), 439–462.
- Mugford, S. T., & Osbourn, A. (2012). Saponin synthesis and function. *Isoprenoid synthesis in plants and microorganisms: new concepts and experimental approaches*, 405–424.
- Mu'nisa, A., Pagarra, H., & Maulana, Z. (2018). Active compounds extraction of cocoa pod husk (*Theobroma cacao* L.) and potential as fungicides. *Journal of Physics: Conference Series*. IOP Publishing
- Mythill, K., Reddy, C. U., Chamundeeswari, D., & Manna, PK. (2014). Determination of Total Phenol, Alkaloid, Flvonoid, and Tannin in Different Extracts of *Calanthe Triplicata*. RESEARCH AND REVIEWS: JOURNAL OF PHARMACOGNOSY AND PHYTOCHEMISTRY, 2(2).
- Nakai, K., & Tsuruta, D. (2021). What are Reactive oxygen species, free radicals, and oxidative stress in skin diseases?. *International journal of molecular sciences*, 22(19), 10799.
- Narendhirakannan, R. T., & Hannah, M. A. (2013). Oxidative stress and skin cancer: an overview. *Indian journal of clinical biochemistry : IJCB*, 28(2), 110–115.
- Nagarajan, J., Ramanan, R. N., Raghunandan, M. E., Galanakis, C. M., & Krishnamurthy, M. P. (2017). Chapter 8 - Carotenoids. *Nutraceutical and Functional Food Components*, 259-296.
- Ogbole, O.O., Segun, P.A. & Adeniji, A.J. (2017). In vitro cytotoxic activity of medicinal plants from Nigeria ethnomedicine on Rhabdomyosarcoma cancer cell line and HPLC analysis of active extracts. *BMC Complement Altern Med* 17, 494.
- Okuda, T., & Ito, H. (2011). Tannins of constant structure in medicinal and food plants—Hydrolyzable tannins and polyphenols related to tannins. *Molecules*, 16(3).
- Olugbami, J. O., Gbadegesin, M. A., & Odunola, O. A. (2014). *In vitro* evaluation of the antioxidant potential, phenolic and flavonoid contents of the stem bark ethanol extract of *Anogeissus leiocarpus*. *African journal of medicine and medical sciences*, 43(Suppl 1), 101–109.
- Panche, A. N., Diwan, A. D., & Chandra, S. R. (2016). Flavonoids: an overview. *Journal of nutritional science*, 5, e47.
- Parbuntari, H., Prestica, Y., Gunawan, R., Nurman, M. N., & Adella, F., Preliminary phytochemical screening (qualitative analysis) of cacao leaves (*Theobroma cacao* L.). *EKSAKTA* 19(2).
- Perluigi, M., Di Domenico, F., Blarzino, C., Foppoli, C., Cini, C., Giorgi, A., Grillo, C., De Marco, F., Butterfield, D. A., Schininà, M. E., & Coccia, R. (2010). Effects of UVB-induced oxidative stress on protein expression and specific protein oxidation in normal human epithelial keratinocytes: a proteomic approach. *Proteome science*, 8, 13.
- Pontis, J. A., Costa, L. A. M. A. D., Silva, S. J. R. D., & Flach, A. (2014). Color, phenolic and flavonoid content, and antioxidant activity of honey from Roraima, Brazil. *Food Science Technology*, 34(1).
- Redza-Dutordoir, M., & Averill-Bates, D. A. (2016). Activation of apoptosis signalling pathways by reactive oxygen species. *Biochimica et Biophysica Acta (BBA) - Molecular Cell Research*, 1863(12), 2977–2992.
- Researchgate. (2013). Re: For DPPH, total antioxidants and lipid peroxidation assay which control to use: Gallic acid or Ascorbic acid?. Retrieved from: <https://www.researchgate.net/post/For-DPPH-total-antioxidants-and-lipid-peroxidation-assay-which-control-to-use-Gallic-acid-or-Ascorbic-acid/51949cd4d039b1bf6f000014/citation/download>.
- Riss, T., Niles, A., Moravec, R., Karassina, N., & Vidugiriene, J. (2019). Cytotoxicity assays: *In vitro* methods to measure dead cells. *Assay Guidance Manual [Internet]*. Retrieved on 18 December 2022 from <https://www.ncbi.nlm.nih.gov/books/NBK540958/>
- Royal Botanic Gardens Kew. (2022). *Litsea oppositifolia* Gibbs | *Plants of the World Online* [Internet]. Retrieved 3 October 2022 from <https://powo.science.kew.org/taxon/urn:lsid:ipni.org:names:465906-1#distributions>



- Rohwer, J. G. (2013). [Indonesia, Java, Bogor Botanic Garden, tree no. XX.A.107, 28 Aug 2013.] [Photograph].  
<https://lauraceae.myspecies.info/category/lauraceae/lauraceae/litsea/litsea-oppositifolia>
- Singh, D., & Chaudhuri, P. K. (2018). Structural characteristics, bioavailability and cardioprotective potential of saponins. *Integrative medicine research*, 7(1), 33–43.
- Swann G. (2010). The skin is the body's largest organ. *Journal of visual communication in medicine*, 33(4), 148–149.
- Ullah, A., Munir, S., Badshah, S. L., Khan, N., Ghani, L., Poulson, B. G., Emwas, A. H., & Jaremko, M. (2020). Important flavonoids and their role as a therapeutic agent. *Molecules (Basel, Switzerland)*, 25(22), 5243.
- US EPA. (2022). *Ultraviolet (UV) Radiation and Sun Exposure | US EPA*. [online] Available at: <<https://www.epa.gov/radtown/ultraviolet-uv-radiation-and-sun-exposure>> [Accessed 3 October 2022].
- Wachsmann, P., & Lamprecht, A. (2012). *Polymeric Nanoparticles for the Selective Therapy of Inflammatory Bowel Disease. Nanomedicine - Cancer, Diabetes, and Cardiovascular, Central Nervous System, Pulmonary and Inflammatory Diseases*, 377–397.
- Wang, P. W., Hung, Y. C., Lin, T. Y., Fang, J. Y., Yang, P. M., Chen, M. H., & Pan, T. L. (2019). Comparison of the biological impact of UVA and UVB upon the skin with functional proteomics and immunohistochemistry. *Antioxidants (Basel, Switzerland)*, 8(12), 569.
- Wilson, B. D., Moon, S., & Armstrong, F. (2012). Comprehensive review of ultraviolet radiation and the current status on sunscreens. *The Journal of clinical and aesthetic dermatology*, 5(9), 18–23.
- Wilson, V. G. (2014). Growth and differentiation of HaCaT Keratinocytes. *Epidermal Cells Methods and Protocols Third Edition*. Humana Press.
- Wong, M. H., Lim, L. F., Ahmad, F. B., & Assim, Z. B. (2014). Antioxidant and antimicrobial properties of *Litsea elliptica* Blume and *Litsea resinosa* Blume (Lauraceae). *Asian Pacific journal of tropical biomedicine*, 4(5), 386–392.
- Wu, Y. K., Tu, Y. K., Yu, J., & Cheng, N. C. (2020). The Influence of Cell Culture Density on the Cytotoxicity of Adipose-Derived Stem Cells Induced by L-Ascorbic Acid-2-Phosphate. *Scientific reports*, 10(1), 104.
- Wulandari, I., Kusuma, I. W., & Kuspradini, H. (2018). Antioxidant and antibacterial activity of *Litsea garciae*. *IOP Conference Series: Earth and Environmental Science*.
- Yousef, H., Alhajj, M., Sharma, S. (2021). Anatomy, Skin (Integument), Epidermis. *Statpearls Internet*. Treasure Island, FL. Statpearls Publishing. Retrieved on 4 October 2022 from <https://www.ncbi.nlm.nih.gov/books/NBK470464/>
- Zakhrifah, Y. M. (2019). *Antioxidant Activity and Total Phenolic Content of Leaves and Stem Bark Extracts of Litsea oppositifolia Gibbs [Indonesian]*. (Thesis, University of Indonesia, Depok, Indonesia)

## APPENDICES

**Table 6.1.** Raw data of the DPPH assay of LO bark extract

<b>Concentrati on (ppm)</b>	<b>7.8125</b>	<b>16.625</b>	<b>31.25</b>	<b>62.5</b>	<b>125</b>	<b>250</b>	<b>500</b>	<b>1000</b>
	29.9340	25.9864	38.4925	43.9627	62.2498	59.1242	71.8737	65.7574
	16.4824	19.2821	32.8930	44.8241	63.8622	63.2161	71.4429	64.5513
	16.9993	20.6174	33.3668	48.5714	66.1881	63.6468	72.5197	67.3941

**Table 6.2.** Raw data of the DPPH assay of ascorbic acid

<b>Concentrati on (ppm)</b>	<b>3.215</b>	<b>6.25</b>	<b>12.5</b>	<b>25</b>	<b>50</b>	<b>100</b>
	29.9340	25.9864	38.4925	43.9627	62.2498	59.1242
	16.4824	19.2821	32.8930	44.8241	63.8622	63.2161
	16.9993	20.6174	33.3668	48.5714	66.1881	63.6468

**Table 6.3.** Raw data of the UVB irradiation optimization

<b>Time (hours)</b>	<b>Control</b>	<b>10 cm</b>	<b>15 cm</b>
3	108.7624904	62.04428841	57.78022583
	87.85549577	58.27707264	57.82153677
	103.3820138	103.2811234	93.63811622
6	94.17213431	47.66899767	49.13937867
	110.4978773	49.71694972	57.7665827
	95.32998842	65.001665	42.52728799
24	108.9585474	9.497251859	7.800829876
	84.78074683	27.85321694	10.40536227
	106.2607057	19.75428387	12.85668688

**Table 6.4.** Raw data of the cytotoxic assay of LO bark extract

<b>Control</b>	<b>6.25</b>	<b>12.5</b>	<b>25</b>	<b>50</b>	<b>100</b>	<b>200</b>
82.5834	167.9725	186.3949	199.1001	174.4839	136.2096	68.5548
120.8576	122.234	207.0408	159.2377	55.532	66.4902	136.2096
96.559	105.7173	147.009	131.9217	153.2028	89.0418	166.702

**Table 6.5.** Raw data of the cytotoxic assay of ascorbic acid

<b>Control</b>	<b>6.25</b>	<b>12.5</b>	<b>25</b>	<b>50</b>	<b>100</b>	<b>200</b>
82.5834	51.0852	100.4764	112.7051	59.9788	45.2091	60.7729
120.8576	101.4293	141.1329	150.0265	82.8481	69.8253	62.9963
96.559	198.4648	127.1572	151.1382	121.5987	63.4727	73.3192

**Table 6.6.** Raw data of the cytoprotective assay of LO bark extract

<b>Control</b>	<b>0</b>	<b>6.25</b>	<b>12.5</b>	<b>25</b>	<b>50</b>	<b>100</b>	<b>200</b>
82.5834	35.5744	52.7498	48.3835	45.8497	45.5448	57.6476	46.8643
120.8576	48.2795	57.5871	45.6123	40.2946	48.7501	62.04	40.8709
96.559	40.3388	60.4809	54.5136	40.8886	53.3525	67.7794	38.6339

**Table 6.7.** Raw data of the cytoprotective assay of ascorbic acid

<b>Control</b>	<b>0</b>	<b>6.25</b>	<b>12.5</b>	<b>25</b>	<b>50</b>
82.5834	35.5744	54.9227	57.0467	76.493	60.7255
120.8576	48.2795	55.5732	57.4857	77.2944	69.3437
96.559	40.3388	59.6501	57.354	72.2572	64.2483